Article:

Olumayegun, O., Wang, M. orcid.org/0000-0001-9752-270X and Oko, E. orcid.org/0000-0001-9221-680X (2019) Thermodynamic performance evaluation of supercritical CO2 closed Brayton cycles for coal-fired power generation with solvent-based CO2 capture. Energy, 166. pp. 1074-1088. ISSN 0360-5442

https://doi.org/10.1016/j.energy.2018.10.127

Thermodynamic Performance Evaluation of Supercritical CO_2 Closed Brayton Cycles for Coal-fired Power Generation with Solvent-based CO_2 Capture

Olumide Olumayegun, Meihong Wang*, Eni Oko

Department of Chemical and Biological Engineering, University of Sheffield, Mappin Street, Sheffield, S1 3JD, United Kingdom

*Corresponding author.

E-mail addresses: o.olumayegun@sheffield.ac.uk (O. Olumayegun), Meihong.Wang@sheffield.ac.uk (M. Wang), e.oko@sheffield.ac.uk (E. Oko)

Abstract

Power generation from coal-fired power plants represents a major source of CO_2 emission into the atmosphere. Efficiency improvement and integration of carbon capture and storage (CCS) facilities have been recommended for reducing the amount of CO_2 emissions. The focus of this work was to evaluate the thermodynamic performance of s-CO_2 Brayton cycles coupled to coal-fired furnace and integrated with 90% post-combustion CO_2 capture. The modification of the s-CO_2 power plant for effective utilisation of the sensible heat in the flue gas was examined. Three bottoming s-CO_2 cycle layouts were investigated, which included a newly proposed single recuperator recompression cycle. The performances of the coal-fired s-CO_2 power plant with and without carbon capture were compared. Results for a 290 bar and 593 ^{0}C power cycle without CO_2 capture showed that the configuration with single recuperator recompression cycle as bottoming cycle has the highest plant net efficiency of 42.96% (Higher Heating Value). Without CO_2 capture, the efficiencies of the coal-fired s-CO_2 cycle plants were about 3.34-3.86% higher than the steam plant and about 0.68-1.31% higher with CO_2 capture. The findings so far underscored the promising potential of cascaded s-CO_2 power cycles for coal-fired power plant application.

Graphical abstract

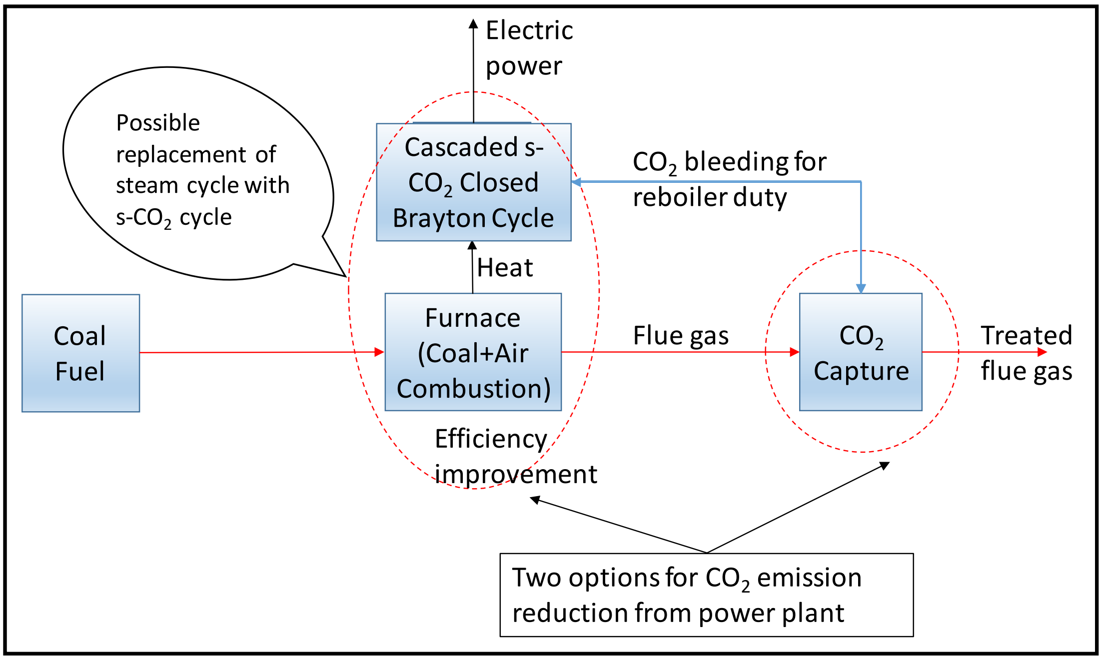

Keywords

Coal-fired power plant;

Supercritical CO_2 Brayton cycle;

Carbon capture;

Chemical absorption;

Process modelling/simulation;

Highlights

- Supercritical CO_2 cycle was investigated for coal-fired power plant application
- Three s-CO_2 cycles were investigated as possible bottoming cycle options
- Integration of coal-fired plant with post-combustion CO_2 capture was studied
- Thermodynamic analysis and performance comparison were performed

Nomenclature and Units

Abbreviations

CCS	carbon capture and storage
ESP	electrostatic precipitator
FD	forced draft
FGD	flue gas desulfurization

HP	high-pressure
HHV	higher heating value
HTR	high temperature recuperator
ID	Induced draft
LP	low-pressure
LTR	low temperature recuperator
MC	main compressor
MEA	monoethanolamine
PA	primary air
PCC	post-combustion CO_2 capture
PSD	particle size distribution
RC	recompression compressor
s-CO_2	supercritical carbon dioxide
TTD	terminal temperature difference
USC	ultra-supercritical

Symbols

C_i	Concentration of the ith component (mol/m^3)
E	Activation energy (J/mol)
HHV	Higher heating value (J/kg)
k	Pre-exponential factor
$\dot{m}$	Mass flow rate (kg/s)
n	Temperature exponent
N	Number of components
P	Power (watt or J/s)
Q	Heat transferred (watt or J/s)
r	Rate of reaction
R	Universal gas constant
T	Temperature (K)
α_i	Exponent of the ith component
η	Efficiency
π	Product operator
Σ	Sum operator

Subscripts

aux	auxiliary
C	Compressor
$elec$	Electrical
gen	Generator
HP	High pressure
i	Component index
LP	Low pressure
MC	Main compressor
RC	Recompression compressor
T	Turbine

1 Introduction

1.1 Background

Coal-fired power plants are still playing a significant role in meeting world energy demands and it is expected to remain a key component of the global energy mix into the future due to its reliability, security of fuel supply, cheap fuel and competitive cost of electricity [1, 2]. However, one prime concern about continued use of fossil fuels like coal is the emission of CO_2 to the atmosphere. Therefore, reducing CO_2 emissions from coal-fired power has become a policy focus in many countries. Two options that have been identified for mitigating CO_2 emissions from fossil fuel power plants are CCS (carbon capture and storage) and efficiency improvement. Post-combustion CO_2 capture (PCC) by chemical absorption with solvent is currently the most preferred CCS option [3, 4]. Efficiency improvement usually requires increased main steam temperature and pressure. Hence, the state-of-the-art technology for coal-fired power generation, the ultra-supercritical (USC) steam plant, now operates at a steam pressure up to 300 bar and temperature up to 600 ^{0}C with reheat [5]. However, CCS systems and efficiency improvement have their limitations. Integration of PCC system with fossil fuel power plants leads to significant efficiency penalty and increased cost of electricity generation. Also, lack of advanced materials to withstand harsh operating conditions limits further improvement in efficiency.

In this paper, to improve the efficiency of coal-fired power plants, supercritical carbon dioxide (s-CO_2) Brayton cycle is considered as an alternative to the conventional steam Rankine cycle. Additionally, CO_2 capture is facilitated by integrating an aqueous monoethanolamine (MEA)-based PCC system with the s-CO_2 cycle power plant. S-CO_2 Brayton cycle has been found to have higher cycle efficiency than steam Rankine cycle and other gas Brayton cycles in the temperature range typically encountered in pulverised coal-fired power plant (450 ^{0}C to 650 ^{0}C) [6-10]. Other potential benefits of s-CO_2 cycle compared to steam cycle include [6, 11-19]:

- Smaller size of the components
- Less complex system layout
- Less risk of corrosion and scaling and no formation of water droplets that could damage the turbine blades [10, 20]
- Reduced water consumption [14, 19]

1.2 Review of s-CO_2 power cycle

A CO_2 closed Brayton cycle was originally patented by Sulzer in 1950 [21]. Later in the 1960s, Feher [10, 22], Angelino [12, 23] and Dekhtiarev [24] all investigated s-CO_2 power cycle. Feher identified CO_2 as a suitable working fluid due to its unique properties such as low critical pressure, good thermal stability at temperature of interest, inertness, availability of property data, and abundant, non-toxic and inexpensive [10]. Angelino concluded that s-CO_2 power cycle has the potential to perform better than reheat steam cycle on account of efficiency, simplicity and compactness [12]. Dekhtiarev [24] studied condensing reheated s-CO_2 cycles as a good alternative to steam cycle for fossil fuel plant [25]. According to recent comprehensive reviews by Olumayegun et al. [26], Ahn et al. [19], Crespi et al. [27] and Li et al. [28], s-CO_2 power cycles are currently being widely investigated as power conversion system for application in nuclear, fossil, concentrated solar power, biomass, and waste heat recovery systems because of its advantages [8, 11, 15, 17, 20, 29-31].

Dostal [11] contributed to renewed interest in s-CO_2 power cycle for nuclear reactor application by providing a detailed analysis based on thermodynamic performance and cost. The study showed that s-CO_2 cycle achieved higher thermal efficiency and reduced cost of power plant compared to steam cycle at 550 ^{0}C turbine inlet temperature. Studies by Pharm et al.[8] concluded that the s-CO_2 recompression cycle in condensing mode is the most fitting configuration for pressurised water reactor (PWR) and sodium-cooled fast reactor (SFR) application. The use of mixture of CO_2 with additive gases to improve the performance of s-CO_2 cycle of a nuclear reactor was investigated by Hu et al. [17]. Even though s-CO_2 cycle is usually viewed to provide superior thermodynamic performance than steam cycle only in the medium to high-temperature range (greater than 450 ^{0}C), Santini et al. [25] investigated the adoption of s-CO_2 cycle for a far lower temperature (about 260 ^{0}C) of an existing PWR. The results indicated that a reheated recompression s-CO_2 cycle achieved a net cycle efficiency of about 34% compared to 33.5% of the existing steam cycle and the plant footprint was 10 times smaller than the steam cycle plant.

For concentrated solar power (CSP), Chacartegui et al. [32] investigated two stand-alone s-CO_2 cycle configurations and a combined cycle (comprising a topping s-CO_2 cycle and a bottoming Organic Rankine Cycle (ORC)) as an alternative to the conventional steam cycle. Preliminary results from the study showed that the s-CO_2 cycles could provide both efficiency and cost benefits. Al-Sulaiman and Atif [33] compared the performance of five different s-CO_2 Brayton cycle configurations for CSP application and the recompression cycle was found to give the best efficiency. Recompression and partial cooling cycles were compared by Neises and Turchi [29] for CSP, highlighting the potential reduction in cost and improvement of CSP receiver efficiency with the partial cooling cycle. Recently, Wang et al. [34] reviewed and compared the main s-CO_2 cycle configurations integrated with molten salt solar power towers having both the main heater and a reheater.

S-CO_2 cycles and the various configurations have also been investigated as bottoming cycles for fuel cell [20] and gas turbine system [15] as well as an alternative power conversion system for other waste heat recovery processes [35, 36] and biomass plants [7]. Bae et al. [20] investigated s-CO_2 cycle configurations comprising an s-CO_2 Brayton-steam Rankine cycle cascade, a recompression cycle and two simple recuperated cycle (a supercritical and a trans-critical cycle) as bottoming cycles for molten carbonate fuel cell. Kim et al. [15] compared the performance of nine s-CO_2 cycle layouts together with three newly developed concept as bottoming cycles for gas turbine plant. It was concluded that although the recompression cycle has a good cycle efficiency, it is not suitable as a bottoming cycle due to its poor heat recovery factor. Small to medium-scale biomass power plant employing either a simple recuperated or a recompression s-CO_2 Brayton cycle as topping cycle and a simple recuperated s-CO_2 Brayton cycle as bottoming cycle was studied by Manente and Lazzaretto [7]. Results of performance optimisation showed that the cascaded s-CO_2 Brayton cycles plant could achieve about 10% higher efficiency than existing biomass plant.

Various researchers have also proposed adaptation of s-CO_2 Brayton cycle as the main/topping cycle for coal-based power plant. However, one problem of such application is the inefficient utilisation of the heat content of the flue gas [16, 30, 31]. Mecheri and Le Moullec [30] investigated the performance of coal-fired s-CO_2 Brayton cycle by comparing the effects of number of reheat and number of recompression, and the effects of advanced flue gas economiser configurations. Heat utilisation was improved by transferring flue gas heat to a fraction of cold CO_2 working fluid taken from the main compressor outlet as well as preheating of combustion air. Results showed that the plant net efficiency was higher than that of supercritical and USC steam plant by 5.3% and 2.4% respectively. Le Moullec [31] presented a conceptual study of coal-fired s-CO_2 Brayton cycle integrated with 90% post-combustion amine-based CO_2 capture unit. Performance improvement entailed the use of double reheat configuration, cold CO_2 bleeding from two locations and two stages of combustion air preheating. Technical and economic evaluation of the plant showed that 15% reduction in levelised cost of electricity and 45% reduction in the cost of avoided CO_2 emission could be achieved. Hanak and Manovic [16] proposed s-CO_2 cycle instead of the conventional steam cycle for electricity generation from the high-grade heat of calcium looping process. Results of retrofitting the calcium looping process with s-CO_2 recompression cycle indicated that a gain in efficiency of about 1-2% over that of the steam cycle could be obtained.

1.3 Aim of this study and its novelties

The aim of this paper is to evaluate the thermodynamic performance of coal-fired s-CO_2 Brayton cycle power plant that has been adapted for efficient utilisation of flue gas heat by using a bottoming s-CO_2 Brayton cycle in conjunction with a main/topping s-CO_2 Brayton cycle. So far, the use of s-CO_2 Brayton cycles as both topping cycle and bottoming cycle of a coal-fired power plant has not been explored in the literature. In this study, a single reheat s-CO_2 recompression cycle was considered as the topping cycle while three simpler s-CO_2 cycle were investigated as possible bottoming cycle for recovering the excess heat in the flue gas exiting the furnace. The investigated bottoming cycle options are simple recuperated cycle, partial heating cycle and a newly proposed concept referred to as single recuperator recompression cycle. Performance evaluation was performed both for s-CO_2 cycle plants without CO_2 capture and for plants with CO_2 capture unit integrated. The performances of the different coal-fired s-CO_2 cycle configurations were compared with reference to a supercritical steam cycle that was chosen as the benchmark. The most promising of the layouts was determined and the effects of cycle parameters such as turbine inlet temperature, precooler outlet temperature/pressure and recuperator's minimum terminal temperature difference (TTD) on the plant performance were investigated. The whole system comprising the coal-fired furnace, the s-CO_2 cycles and the MEA-based PCC plant were modelled and simulated with Aspen Plus software.

2 Process configurations and description

2.1 Supercritical CO_2 closed Brayton cycle

A unique feature of CO_2 as working fluid is that its critical pressure (7.3773 MPa) and temperature (30.978 °C) are easily achievable. The properties of CO_2 vary rapidly around the critical point and the density is greatly increased. Hence, s-CO_2 cycles take advantage of the increased density by operating the compressor inlet close to the critical point so that the compression work is significantly reduced. The reduced compression work thus enables the achievement of high thermodynamic efficiency.

The baseline closed Brayton cycle is the simple recuperated cycle. The layout and T-S diagram of a simple recuperated s-CO_2 Brayton cycle are shown in Figure 1a. It consists of a heat source (1 – 2), a turbine (2 – 3), a recuperator (3 – 4 & 6 – 1), a precooler (4 – 5) and a compressor (5 – 6). Though the rapidly varying fluid properties around the critical point is a feature that facilitates the reduced compression work of s-CO_2 cycle, it also prevents effective heat transfer in the recuperator of simple recuperated s-CO_2 cycle. This is due to mismatch of specific heat capacity between the high-pressure CO_2 in the cold side and the low-pressure CO_2 in the hot side of the recuperator. This could lead to temperature cross over in the recuperator (the so-called "pinch point problem") and consequently, the cold stream cannot be preheated high enough to achieve good recuperator effectiveness. Hence, it is difficult to achieve high efficiency in simple recuperated s-CO_2 cycle even with the conventional methods of enhancing efficiency such as reheating and intercooling because of the excessively low effectiveness of the recuperator [37].

Other complex layouts have been suggested in the literature to minimise the detrimental effects of the differences in heat capacities [10-12, 15, 19, 38]. Of all the layouts, the recompression s-CO_2 cycle (Figure 1b) is generally considered the most promising with the highest thermodynamic efficiency and a relatively simpler configuration than most others [11]. A component count of the different layouts by Kim et al. [15] showed that only the simple recuperated (Figure 1a) and the partial heating cycle (Figure 1c) is simpler (fewer components) than the recompression cycle. Hence, this study considered only the simple recuperated cycle, the recompression cycle and the partial heating cycle. However, an additional new cycle concept referred to as single recuperator recompression s-CO_2 cycle (Figure 1d) was proposed. The newly proposed layout has one component less than the recompression cycle and just one component more than the simple cycle. This configuration has been investigated previously in an initial study by the authors [39]. Conboy et al. [40] suggested a similar but more complex cycle layout for geothermal heat application.

In the recompression cycle (Figure 1b), the recuperator is separated into two: the high-temperature recuperator (HTR) and the low-temperature recuperator (LTR). The problem of heat capacity mismatch is resolved by splitting the flow into two streams at point 5. The main stream is cooled in the precooler (point 5 to point 6) to the main compressor (MC) inlet temperature. The second stream is compressed directly in the recompressing compressor (point 5 to point 9) and mixed with the main flow at the exit of the LTR cold stream (point 8) before entering the cold side of the HTR (point 10). The flow split fraction can be adjusted to make the heat capacity (i.e. the product of mass flow rates and specific heat capacity) of CO_2 on the high-pressure side of the LTR the same as that of the low-pressure side CO_2. Hence, with an optimal selection of flow split fraction, high recuperator effectiveness and consequently high thermodynamic efficiency can be achieved. The layout, as well as T-S diagram of partial heating cycle, is shown in Figure 1c. Matching of the heat capacities of the recuperator streams is achieved by splitting the flow at the compressor outlet (point 6) after compressing the fluid to the maximum cycle pressure in the compressor (point 5 to 6). The new concept, the single recuperator recompression cycle is shown in Figure 1d. It is similar to the recompression cycle except that the HTR was eliminated leaving only one recuperator. The flow is split into two streams at point 4, just like the recompression cycle. This permits the advantage associated with splitting the flow, that is, a balance of the heat capacity between the cold stream and the hot stream of the recuperator.

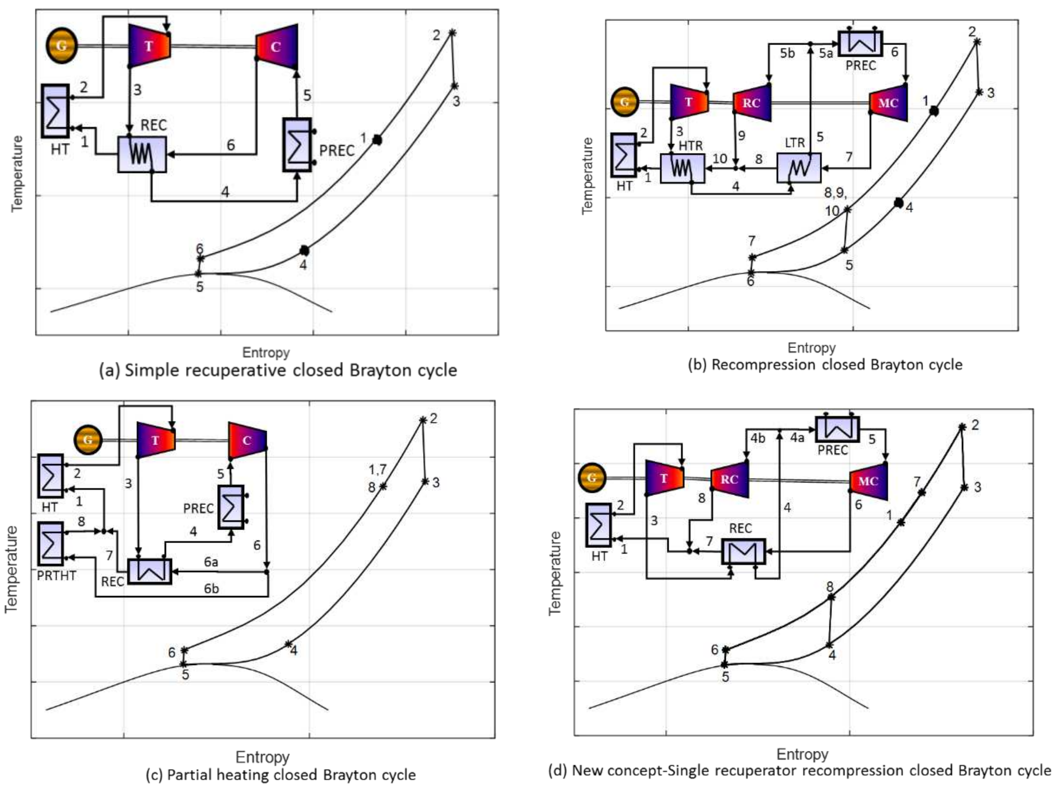

Figure 1 Layout and T-S diagrams of simple recuperative, recompression, partial heating and single recuperator recompression s-CO_2 closed Brayton cycles [18-20, 22]

2.2 Supercritical CO_2 Brayton cycles for pulverised coal-fired application

2.2.1 Coal-fired furnace and the main s-CO_2 closed Brayton cycle

Integration of the main/topping s-CO_2 cycle with the coal-fired furnace is shown in Figure 2. A recompression s-CO_2 cycle was adopted due to its superior performance when compared to other s-CO_2 cycle layouts. The performance is further improved with a single stage of reheat. Preheated CO_2 coming from the HTR entered the furnace at point T1 and exit at T2 after being heated to the maximum cycle temperature. The hot working fluid is expanded in the high-pressure (HP) turbine and returned to the furnace at point T3 for reheating. The reheated CO_2 exiting the furnace at T4 is finally expanded in the LP turbine. During each pass through the furnace, the CO_2 working fluid is heated in three steps: convective economiser (ECOHT/ECORHT), radiant heater (RADHT/RADRHT) and final convective heater or reheater (CHT/CRHT).

Radiant section of the furnace contains the two radiant heaters while the convective section contains the four convective heaters. Approximately half of the heat transferred to the CO_2 is through radiation from the flame to the radiant heaters. Combustion products rise to the top of the furnace and entered the convection zone at point A. The temperature of the hot flue gases at A was maintained at 1010 ^{0}C so that it was below ash softening temperature [41]. As the flue gases flow through the convective section, they are first used for final heating of CO_2 to turbine inlet temperature in the convective heater and reheater. Then CO_2 leaving the HTR and HP turbine are heated in the economisers to the radiant heaters inlet temperature. The flue gases leave the furnace at point B. The CO_2 entering the furnace at T1 is at a higher temperature (about 465 ^{0}C) than the usual feedwater temperature in conventional coal-fired steam boiler (about 260 ^{0}C) [42]. This is due to the high level of recuperation in recompression cycle. Consequently, the flue gases leave the furnace at relatively high temperature (about 495 ^{0}C) in the coal-fired s-CO_2 cycle power plant.

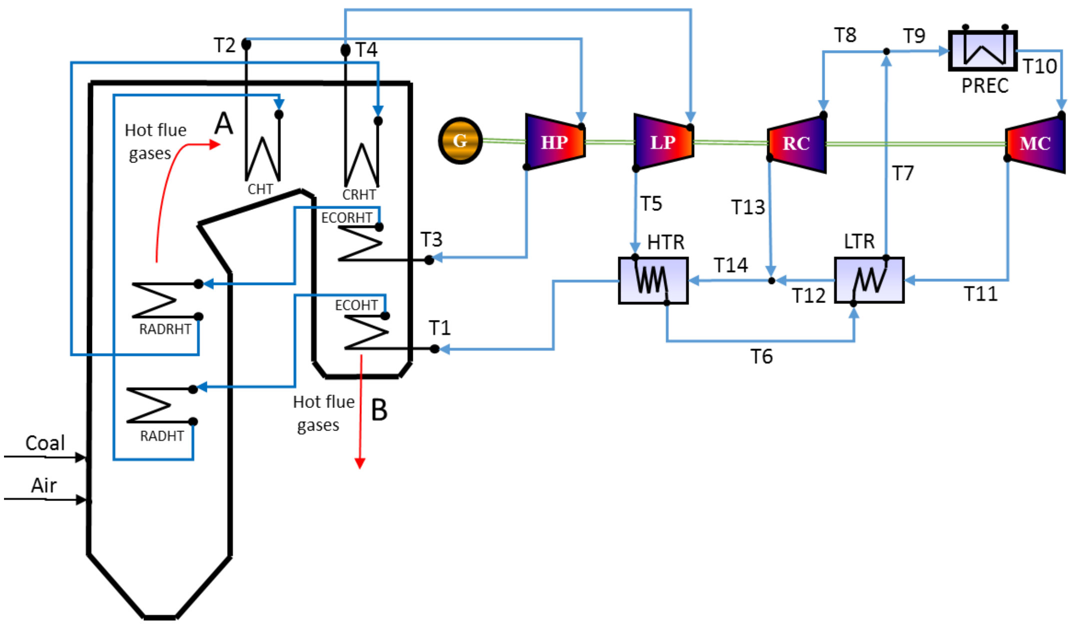

Figure 2 Main single reheat recompression cycle integration with coal-fired furnace

2.2.2 Utilisation of flue gases residual heat

A major drawback of coupling closed Brayton cycle to coal-fired furnace is the significant loss of heat through the hot flue gases leaving the furnace. If this exiting flue gases are not utilised, it will represent the main cause of inefficiency in the power plant [41]. Several options exist for utilising waste heat of flue gases. The first option is to use the flue gases to produce steam or hot water for industrial use or district heating in a combined heat and power (CHP) system. In fact, some of the early-operated coal-fired closed Brayton cycle plants such as the Oberhausen and Kashira plants were used to generate electricity as well as to produce heat for district heating [43]. Secondly, the hot flue gases can be used to preheat part or all of the cycle working fluid prior to the main heat addition in the furnace. Mecheri and Le Moullec [30] employed this option by transferring the flue gases heat to a fraction of CO_2 flow that is extracted from the MC outlet. A third option is to add a bottoming cycle that uses the flue gases high-grade heat to generate additional electrical power [7, 15]. For instance, Echogen (USA) is in the process of commercialising s-CO_2 bottoming power cycle utilising waste heat [44]. The final option is to use the flue gases to preheat the incoming combustion air. This is a common practice in conventional coal-fired power plants.

In this study, the use of bottoming cycle in conjunction with combustion air preheating was selected. In bottoming cycles, the net electric efficiency is a function of not just cycle efficiency (ratio of net electric power produced to heat transferred to the cycle) but also of the heat recovery factor (ratio of recovered heat to available heat in the flue gas) [15]. Closed Brayton s-CO_2 cycle has favourable cycle efficiency. However, when used as a bottoming cycle, the heat recovery in the heater is limited by the high temperature of CO_2 leaving the recuperator [15]. However, the addition of air preheater downstream of the bottoming cycle will help to improve the plant's overall heat recovery factor. Recompression cycle was not used as bottoming cycle in this study. Cycles with simpler layouts and better heat recovery factor were favoured. Hence, the simple recuperated cycle, the partial heating cycle and the newly proposed single recuperator recompression cycle were considered as bottoming cycles in cascade with the main/topping single reheat recompression s-CO_2 cycle.

2.2.3 Overall plant configurations and its integration with PCC

In this study, three coal-fired s-CO_2 cycle configurations (Figure 3, Figure 4 and Figure 5) representing three different bottoming cycle choices were investigated:

- Case A: the simple recuperated s-CO_2 cycle was selected as bottoming cycle as shown in Figure 3
- Case B: shown in Figure 4, the bottoming cycle is the partial heating s-CO_2 cycle
- Case C: the new concept, the single recuperator recompression s-CO_2 cycle was used as the bottoming cycle (Figure 5)

In all the cases, the topping cycle remains the single reheat recompression s-CO_2 cycle integrated with coal-fired furnace. Coal is pulverised to fine powder in the mill. Secondary air, which is a large proportion of the incoming air, is sent to the forced draft (FD) fan while the remaining incoming air goes to the primary air (PA) fan. Air from the PA fan and FD fan is heated in the air preheater thereby recovering part of the remaining heat content of the flue gas exiting the bottoming cycle heater at point C. The heated primary air goes to the mill/pulveriser for drying and conveying the pulverised coal to the burners in the furnace. The heated secondary air is also introduced into the burners, where the coal and the air are mixed and combustion takes place. Heat released from the combustion is transferred to the CO_2 working fluid in the radiant and convective heaters.

The cooled flue gas leaving the air preheater passes through fabric filters or electrostatic precipitator (ESP) for particulate matters (majorly ash) removal. An induced draft (ID) fan increases the flue gas pressure to provide suction to the flue gas in the furnace and for the flue gas to pass through the flue gas desulfurization (FGD) unit. The cleaned flue gas leaving the FGD unit is finally sent either to the PCC unit to remove the CO_2 in the flue gases or directly to the stack.

The s-CO_2 Brayton cycle will need to be altered when a PCC unit is added. In the conventional coal-fired plant, low pressure saturated steam from steam turbine is used for solvent regeneration in the PCC unit. However, in the coal-fired s-CO_2 Brayton cycle plant, sensible heat of the CO_2 working fluid is used for solvent regeneration. Hence, each of the three cases is integrated with the PCC unit as shown in Figure 6. Hot CO_2 from the HTR hot stream outlet is conveyed to the reboiler of the PCC unit. The CO_2 is then returned to the s-CO_2 cycle at the LTR hot stream outlet after supplying the required reboiler duty. The flue gas from the power plant is stripped of its CO_2 before being sent to the stack. A detailed description of the PCC unit is provided in Section 4.

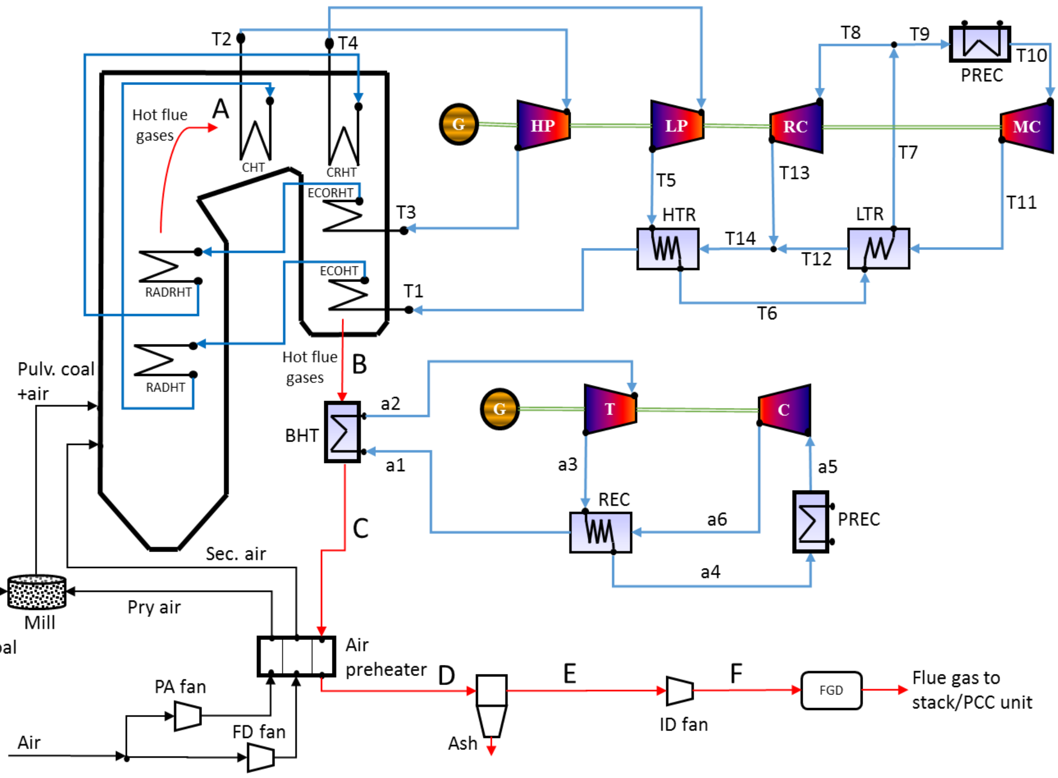

Figure 3 Case A - Simple recuperative bottoming cycle

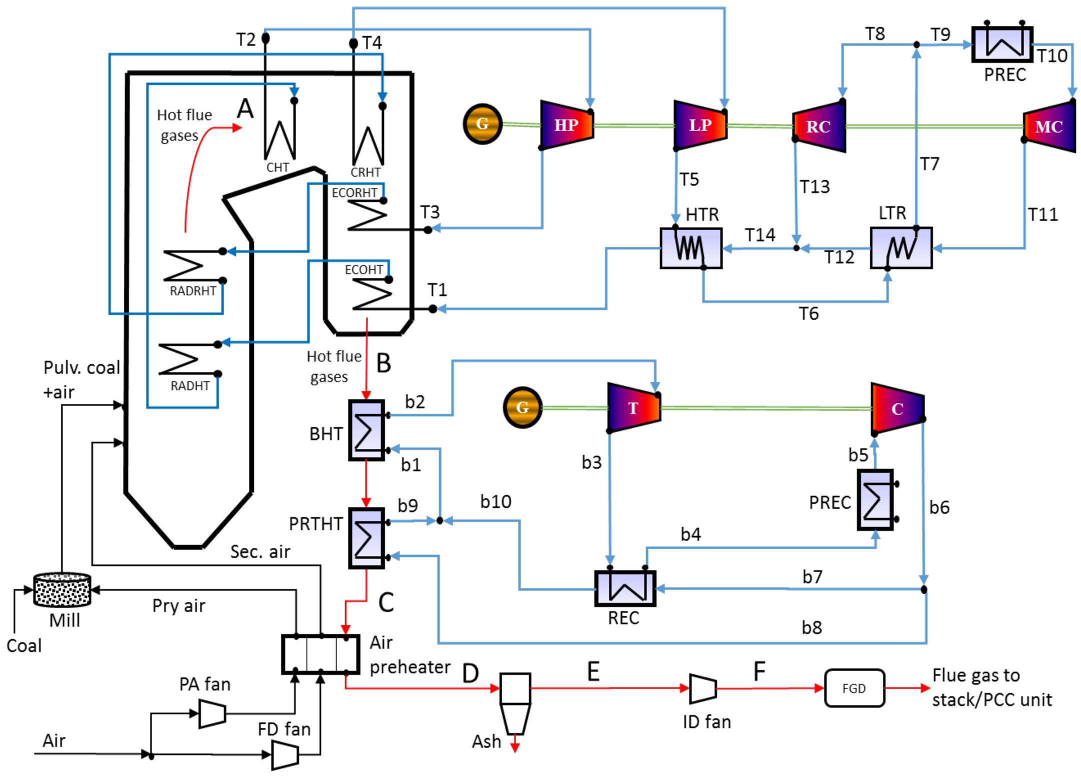

Figure 4 Case B - Partial heating bottoming cycle

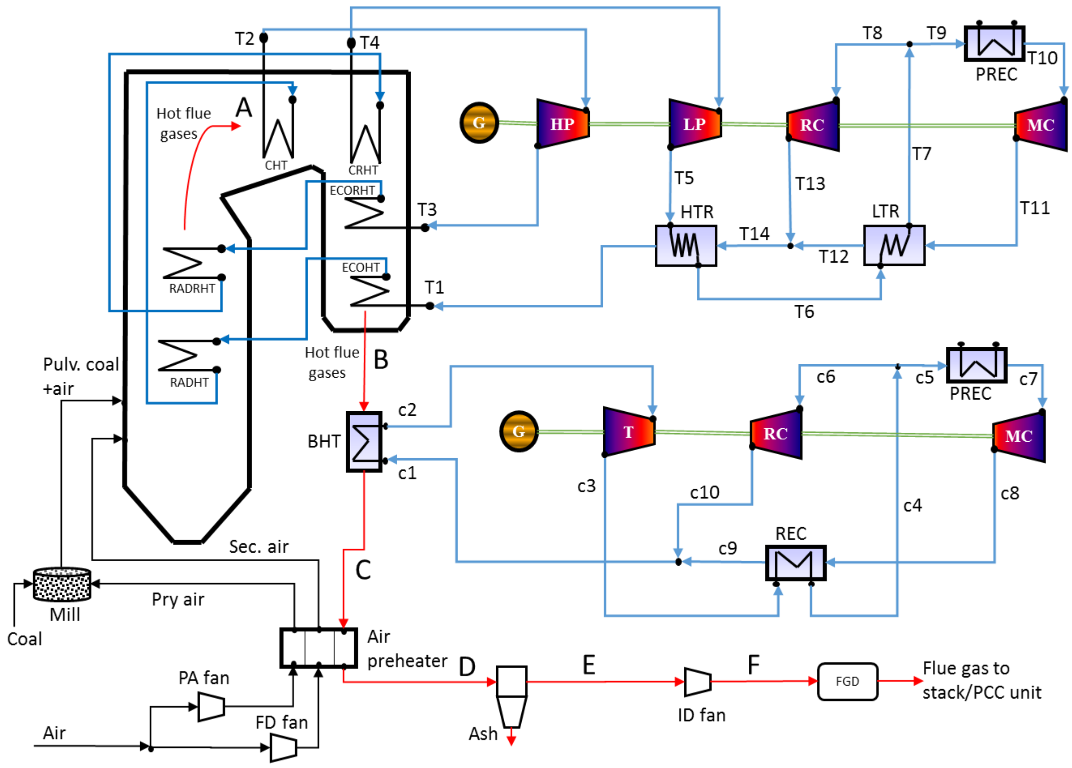

Figure 5 Case C - Single recuperator recompression bottoming cycle

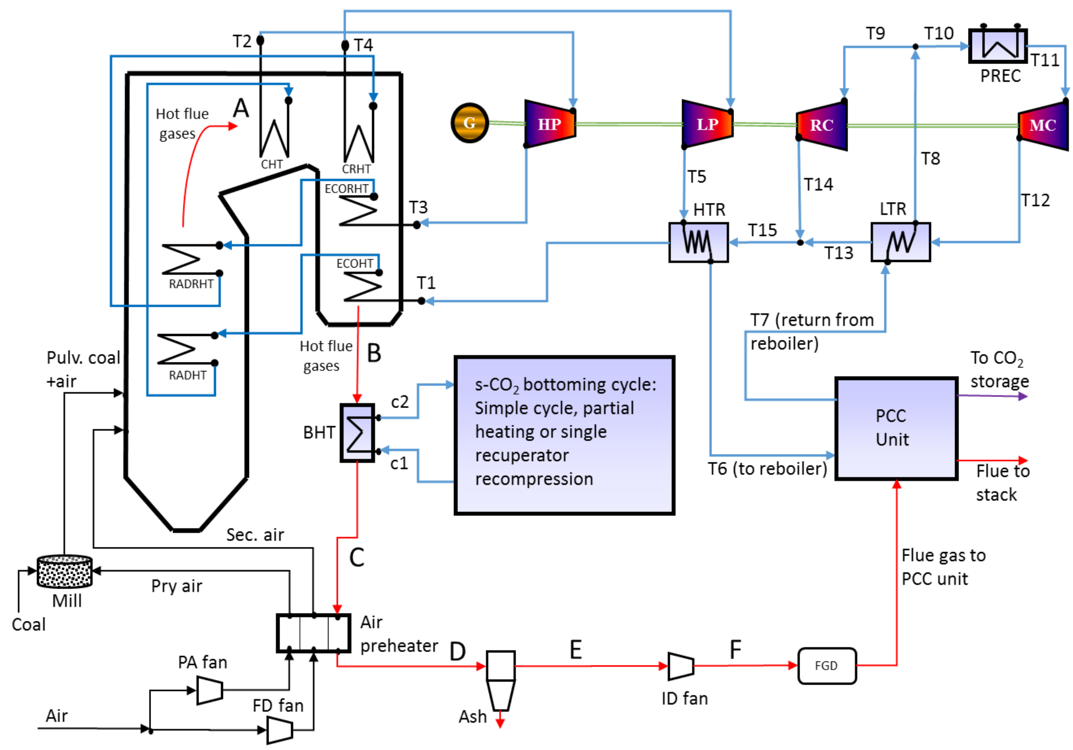

Figure 6 Integration of coal-fired s-CO_2 Brayton cycle with PCC unit

3 Steady state modelling in Aspen Plus®

A model of the three cases of coal-fired s-CO_2 cycle power plant with PCC was developed for performance comparison among the cases as well as comparison with a benchmark coal-fired supercritical power plant with 90% CO_2 capture. The benchmark plant was not modelled in this study but the performance results were obtained from Olaleye et al. [45]. A simplified block diagram of the modelled coal-fired s-CO_2 cycle power plant is shown in Figure 7

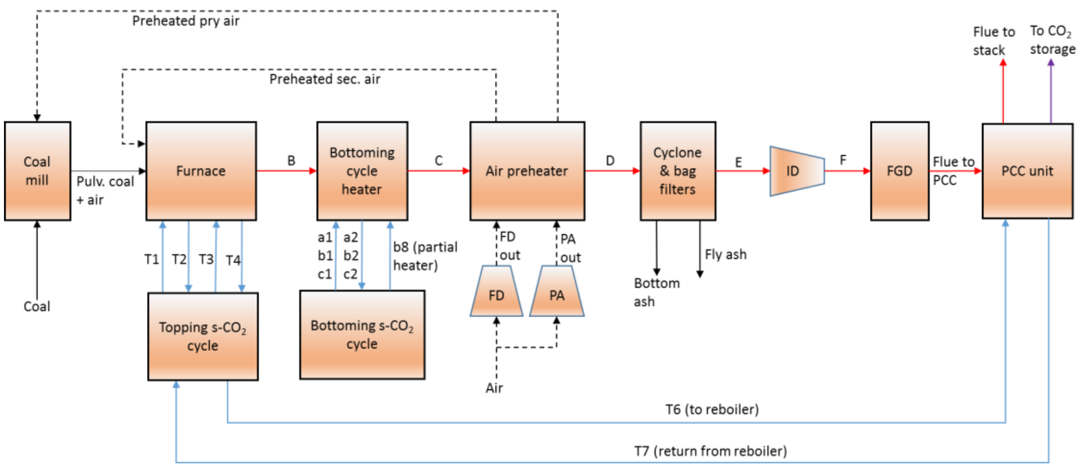

Figure 7 Simplified block diagram of the coal-fired s-CO_2 cycle power plant

3.1 Aspen Plus® software and thermo-physical property methods

The steady state models were implemented with Aspen Plus® V8.4 software to simulate the performance of the coal-fired s-CO_2 cycles power plants. The simulation environment is very flexible for describing the power plant components and connections. The plant components modelled include coal mill, fans, preheaters, pulverised coal-fired furnace, ash removal components, flue gas desulfurization and s-CO_2 cycle components like the external heat sources, turbine, compressor, recuperator and precooler. Description of the PCC structure and its modelling are left until the next section.

Concomitant with process simulation is the need for accurate physical property data and models [46]. Aspen Plus® contains extensive property calculation methods for the physical, chemical and thermodynamic properties of different solid, liquid and gaseous substances. In Aspen Plus®, coal and ash were modelled as nonconventional solids. The HCOALGEN and the DCOALIGT physical property models were used to calculate the enthalpy and density of coal and ash [47]. Peng-Robinson equation of state with Boston Mathias modification (PR-BM) was used to estimate the properties of air and combustion products. For the s-CO_2 properties, REFPROP property package in Aspen Plus® was used. REFPROP has been reported to be accurate and widely applicable to a variety of pure fluid and mixtures [48, 49].

3.2 Coal combustion and furnace modelling

The coal type fired is the Illinois No 6 bituminous coal. Details of the ultimate and proximate analysis of the coal are given in Table 1. The higher heating value (HHV) of the coal was calculated from the ultimate analysis by using the Dulong and Petit formula [50]:

$$HHV\left({}^{MJ}/_{kg}\right) = 33.83C + 144.45\left(H - \frac{O}{8}\right) + 9.38S \tag{3.1}$$

Where C, H, O and S are mass fractions of carbon, hydrogen, oxygen and sulphur in coal respectively.

Incoming air was assumed to consist of nitrogen (76.8 wt.%) and oxygen (23.2 wt.%) at 15 ^{0}C and 1.01 bar. Percent excess air supplied was specified to be 20%. A user-defined Fortran subroutine calculator was implemented to calculate the flow rate of air required for combustion based on the specified percent excess air, the coal flow rate and the coal characteristic. About 23.5% of the incoming air was sent to the PA fan while the rest was sent to the FD fan as secondary air. By specifying the isentropic efficiencies of the fan, the inlet conditions and the discharge pressure, Aspen Plus® determined the power required by the fans. Coal is dried with preheated PA and grounded to fine powder in the coal mill. Volatile matter may be distilled off from the coal in addition to moisture if the temperature of the PA is too high, which may lead to fire hazard [50]. Therefore, the primary air was only preheated to about 215 ^{0}C so that after drying the coal the temperature at pulveriser outlet was within the allowable pulveriser outlet temperature of 75 ^{0}C.

The drying process was modelled with RStoic block. Wet coal and hot PA streams were fed to the RStoic block. The block was used to model drying by converting a portion of the coal to form water. The outlet, which is a stream of dried coal and moist air, is fed to the pulverising mill. The milling process was modelled with a combination of crusher and screen. The crusher was modelled by specifying the outlet particle size distribution (PSD) of coal. The screen block was used to separate the coarse material from the fine material. The coarse portion was returned to the crusher for further grinding. The PSD of the pulverised coal was specified such that about 70% of coal will pass through a 200-mesh screen and less than 1.3% retained on the 50 mesh. The pulverised coal is then conveyed with the PA to the furnace.

In the furnace, the pulverised coal and PA are mixed with the heated secondary air for combustion. A sequence of RYield and RGibbs Aspen Plus® built-in reactor models were used to simulate combustion of coal. RGibbs models chemical equilibrium and phase equilibrium by minimising the Gibbs free energy of the system. Therefore, there was no need to specify the reaction stoichiometry, only a list of possible products may be specified. However, Gibbs free energy can only be calculated for conventional components. Since coal was specified as a nonconventional component, it was first decomposed into its constituent elements by the RYield block. A calculator block was used to determine the actual yield distribution based on the inlet coal attributes. The products of the decomposition together with the heat of reaction associated with the decomposition was then passed to the RGibbs block.

During combustion, the chemical energy in the coal is converted to heat energy, which is transferred to the CO_2 working fluid. Heat radiation from the centre of the flame and absorption of the radiant heat by the working fluid were modelled with HEATER blocks. The radiant heat was divided in the ratio 0.65/0.35 between the main radiant heater and the reheat radiant heater. The exit of the radiant heat source corresponds to the top of the furnace and entrance to the convective zone where the flue gases temperature was maintained at 1010 ^{0}C. Convective heaters in this zone comprising of two final CO_2 heaters and two economisers were modelled with HEATX blocks with flue gases as the hot stream and CO_2 as the cold stream. For a given coal flow rate, a design specification was defined in Aspen Plus® to determine the topping cycle CO_2 flow rate required to cool the flue gases such that a 30 ^{0}C minimum temperature difference was maintained between the flue gases leaving the furnace at point B and CO_2 entering the furnace at point T1.

Table 1 Proximate and ultimate analysis of Illinois No 6 coal [42]

Parameter	**Weight %**
Proximate Analysis (as received)	
Moisture	11.12
Ash	9.70
Volatile matter	34.99
Fixed carbon	44.19
Total	100
Ultimate Analysis (as received)	
Moisture	11.12
Carbon	63.75
Hydrogen	4.50
Nitrogen	1.25
Chlorine	0.29
Sulphur	2.51
Ash	9.70
Oxygen	6.88
Total	100

3.3 Modelling of s-CO_2 closed Brayton cycles

The topping and bottoming s-CO_2 cycles have the same maximum cycle pressure of 290 bar corresponding to the maximum cycle pressure of the benchmark supercritical steam turbine cycle [45]. Similarly, the topping cycle HP and LP turbines inlet temperature were fixed at 593 ^{0}C. Both topping and bottoming cycles' compressor inlet temperature and pressure were fixed just above the critical point at 31 ^{0}C and 76 bar. The bottoming cycle' turbine inlet temperature was fixed at 465 ^{0}C, which is 30 ^{0}C below the flue gas temperature entering the bottoming cycle heater. The values of recuperator's minimum TTD, compressor and turbine isentropic efficiencies, and heat exchanger pressure losses were selected based on values reported in literature. Hence, a minimum TTD of 10℃ was specified for the recuperators [30]. Main compressor, recompression compressor and turbine isentropic efficiencies were 90%, 89% and 93% respectively [30]. Heat exchanger relative pressure losses were fixed at 0.5% [15]. For cycles with split flows, the split fractions could be independently adjusted to obtain optimum cycle efficiency.

Compressors and turbines were simulated in Aspen Plus® with COMPR block. Aspen Plus® calculates the power required (or delivered) based on the inlet conditions, discharge pressure and efficiency. Recuperators were modelled with HEATX block while precoolers were modelled with HEATER blocks. In the bottoming cycle, design specification was used to determine the needed CO_2 flow rate based on a minimum temperature difference of 30 ^{0}C between the flue gas leaving the bottoming cycle heater and the CO_2 entering the heater.

3.4 Preheater, ash removal and flue gas desulfurization

Air preheater was modelled with MHeatX block, which represents heat transfer between the hot flue gases leaving the bottoming cycle heater and two cold streams (i.e. PA and SA). Outlet specifications must be given for two of the three streams. PA and flue gas outlet temperatures were specified. Flue gas outlet temperature of 116 ^{0}C specified for the benchmark steam plant was assumed. Then, an overall energy balance determines the unspecified outlet temperature of the secondary air.

Ash removal from the flue gas was modelled with cyclone and bag filter blocks. 20% of ash was removed as bottom ash by the cyclone while the remaining 80% was removed as fly ash by bag filters. The ash-free flue gas is pushed through the FGD unit by ID fan. The power required by the fan was determined based on its discharge pressure and isentropic efficiency. The FGD removed sulphur oxide in the flue gas before entering the PCC unit.

3.5 Performance calculation

MS Excel™ spreadsheets were used to carry out the performance calculations. Therefore, the MS Excel™ was linked with Aspen Plus® to access simulation results.

Two important performance indicators are the furnace (or heat recovery) efficiency and the cycle efficiency. The furnace efficiency is an indication of the ability of the power cycle to receive the heat available in the heat source while cycle efficiency indicates the ability to convert the received heat into electrical power [7]. The furnace efficiency, $\eta_{furnace}$ is calculated by taking the total amount of heat transferred to the s-CO_2 cycles and dividing it by the coal fuel power supplied to the plant.

$$\eta_{furnace} = \frac{(Q_{cycle})_{top} + (Q_{cycle})_{bottom}}{\dot{m}_{coal}(HHV)} \tag{3.2}$$

Where $(Q_{cycle})_{top}$ is the sum of the heat transferred to the topping s-CO_2 cycle through the economisers, radiant heaters and final convective heater/reheater, $(Q_{cycle})_{bottom}$ is the heat input from flue gases to the bottoming s-CO_2 cycle, $\dot{m}_{coal}$ is the mass flow rate of coal and HHV is the higher heating value of the supplied coal.

Cycle efficiency, η_{cycle}, is calculated by taking the electrical power output of the cycle and dividing by the heat transferred to the cycle. Hence, cycle efficiency for the toping cycle,$(\eta_{cycle})_{top}$, is

$$(\eta_{cycle})_{top} = \frac{(P_{elec})_{top}}{(Q_{cycle})_{top}} \tag{3.3}$$

Where $(P_{elec})_{top}$ is the topping cycle electrical power output given as:

$$(P_{elec})_{top} = \left[\left(\sum P_T\right)_{top} - \left(\sum P_C\right)_{top}\right]\eta_{gen} = (P_{HP} + P_{LP} - P_{MC} - P_{RC})\eta_{gen} \tag{3.4}$$

$\left(\sum P_T\right)_{top}$ is the sum of topping cycle turbine power, $\left(\sum P_C\right)_{top}$ is the sum of topping cycle compressor power, P_{HP} is the HP turbine power, P_{LP} is the LP turbine power, P_{MC} is the main compressor power, P_{RC} is the RC power and η_{gen} is the electrical generator efficiency.

Cycle efficiency for the bottoming cycle is

$$(\eta_{cycle})_{bottom} = \frac{(P_{elec})_{bottom}}{(Q_{cycle})_{bottom}} = \frac{[(\sum P_T)_{bottom} - (\sum P_C)_{bottom}]\eta_{gen}}{(Q_{cycle})_{bottom}} \tag{3.5}$$

Where $(P_{elec})_{bottom}$ is the bottoming cycle electrical power output, $(\sum P_T)_{bottom}$ is the sum of bottoming cycle turbine power and $(\sum P_C)_{bottom}$ is the sum of bottoming cycle compressor power.

The overall cycle efficiency, $\eta_{overall\ cycle}$ is the ratio of the total electrical power output from the cycles, $(P_{elec})_{total}$ to the total heat transferred to the cycles, $(Q_{cycle})_{total}$.

$$\eta_{overall\ cycle} = \frac{(P_{elec})_{total}}{(Q_{cycle})_{total}} = \frac{(P_{elec})_{top} + (P_{elec})_{bottom}}{(Q_{cycle})_{top} + (Q_{cycle})_{bottom}} \tag{3.6}$$

The net power output of the plant, P_{net} is the total or gross power output from the topping and bottoming cycles, $(P_{elec})_{total}$ minus the auxiliary power consumption, P_{aux} in pumps, fans, coal mill etc.:

$$P_{net} = (P_{elec})_{total} - P_{aux} \tag{3.7}$$

The plant net efficiency, η_{net} is defined as the ratio of the net power output to the coal fuel energy input to the plant:

$$\eta_{net} = \frac{P_{net}}{\dot{m}_{coal}(HHV)} \tag{3.8}$$

The three cases in this study with different bottoming cycle options will present different cycle efficiencies and furnace efficiencies. Therefore, the overall impact of the choice of power plant configurations on the plant net efficiency can only be determined through performance calculations and comparison among the cases.

4 Solvent-based post-combustion CO_2 capture

This section discusses the PCC, which is based on chemical absorption through MEA solvent. Benefits of MEA-based PCC include (1) high separation selectivity; (2) It operates at atmospheric conditions; (3) Experimental/pilot plant data are available.

4.1 Description of MEA-based CO_2 capture process

Figure 8 shows a simplified process flow diagram for a typical chemical absorption CO_2 capture process. The main components are absorber, stripper with a reboiler and a condenser attached, direct contact cooler (DCC), rich MEA pump, lean MEA pump, lean/rich cross heat exchanger and lean MEA cooler.

Flue gas from the power plant's FGD unit is first cooled in the DCC to a suitable temperature for absorption (about 40 ^{0}C). The cooled flue gases are introduced into the absorber at the bottom while the lean MEA solvent solution enters the absorber at the top. The flue gases flow upward while the MEA solvent solution flows down under gravity through the absorber (packed column). Chemical absorption of CO_2 in the flue gases by the MEA solvent takes place during the counter-current flow in the absorber. Treated flue gases leave the absorber at the top. Rich MEA solvent (i.e. with higher loading of CO_2) leaves the absorber at the bottom. Its pressure is then increased by the rich MEA pump and heated in the lean/rich cross heat exchanger before entering the stripper at the top. In the stripper column, the rich MEA solvent is stripped of the CO_2 by the application of heat energy in the reboiler. The water vapour and CO_2 mixture released in the stripper is sent to the stripper condenser, which cools the mixture thereby turning most of the water vapour to liquid water. The condensed water and CO_2 are separated in the flash drum. The condensed water is returned back to the stripper while the separated CO_2 leaves the stripper at the top. The resulting lean MEA solvent (i.e. with lower loading of CO_2) exits the stripper at the bottom. The lean MEA solvent leaving the stripper is used to heat the rich MEA solvent in the cross heat exchanger and the temperature is further reduced in the lean MEA cooler before being returned to the absorber column at the top.

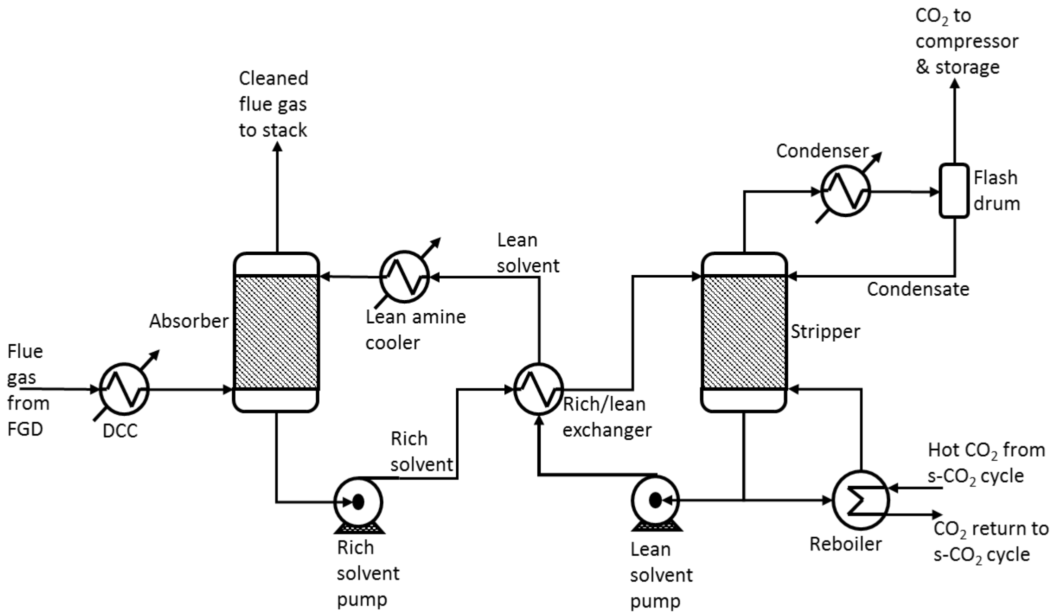

Figure 8 Simplified process flow diagram for MEA-based post-combustion CO_2 capture unit [3]

4.2 Rate-based simulation of the CO_2 capture system in Aspen Plus®

The MEA-based PCC was simulated in Aspen Plus® to determine the performance. The simulation was based on the parameters reported for the benchmark supercritical steam plant's PCC unit, which was validated with data from University of Kaiserslautern pilot plant by Olaleye et al. [45]. The PCC used a 30 wt.% MEA solution as solvent. The temperature of the flue gas and the lean MEA entering the absorber was 40 ^{0}C. Absorber operating pressure was 1.013 bar. The rich MEA solution was heated up to 106 ^{0}C in the cross heat exchanger. The stripper was operating at a pressure of 1.9 bar and the reboiler temperature was maintained at about 120 ^{0}C to avoid thermal degradation of the amine solvent. In Aspen Plus®, RadFrac block was used to model the absorber and the stripper. Koch FLEXIPAC® 1Y structured packing was selected for the absorber and stripper. Previously, the MEA-based PCC model has been validated and scaled up to match the flue gas flow rate of the supercritical power plant by Olaleye et al. [45]. For the plant with 1402 MW of heat input, the design of the absorber and stripper arrived at four absorber columns with a diameter of 5.41m each and three stripper column with a diameter of 4.62m each in order to maintain the columns diameters within the structural limit. Fifteen equilibrium stages were required for each of the absorber and the stripper column.

Modelling of the absorber and stripper in Aspen Plus® was through the use of rate-based models. Rate-based model provides a rigorous and good prediction of the simulation over a wide range of operating conditions unlike the traditional equilibrium-stage modelling approach [51]. The Electrolyte Non-Random-Two-Liquid (ElecNRTL) activity coefficient property package was selected to accurately predict the ionisation equilibrium and the heats of solution of the MEA-CO_2-H_2O system. The solution chemistry of the MEA-based chemical absorption process can be represented by the following equilibrium reactions (R1-R5) [52]:

Water dissociation:	$2H_2O \leftrightarrow OH^- + H_3O^+$	R1
CO_2 hydrolysis:	$CO_2 + 2H_2O \leftrightarrow HCO_3^- + H_3O^+$	R2
Bicarbonate dissociation:	$HCO_3^- + H_2O \leftrightarrow H_3O^+ + CO_3^{2-}$	R3
Carbamate hydrolysis:	$MEACOO^- + H_2O \leftrightarrow MEA + HCO_3^-$	R4
MEA protonation:	$MEAH^+ + H_2O \leftrightarrow MEA + H_3O^+$	R5

Reaction models for the absorber and stripper consist of three equilibrium rate-based controlled reactions, R1, R3 and R5, in conjunction with the following kinetic rate-based controlled reactions (R6-R9) [52]:

Bicarbonate formation (forward):	$CO_2 + OH^- \rightarrow HCO_3^-$	R6
Bicarbonate formation (reverse):	$HCO_3^- \rightarrow CO_2 + OH^-$	R7
Carbamate formation (forward):	$MEA + CO_2 + H_2O \rightarrow MEACOO^- + H_3O^+$	R8
Carbamate formation (reverse):	$MEACOO^- + H_3O^+ \rightarrow MEA + CO_2 + H_2O$	R9

The kinetic reaction rates, r, are described in Aspen Plus® by the power law expression:

$$r = kT^n exp\left(-\frac{E}{RT}\right)\prod_{i=1}^{N} C_i^{a_i} \tag{4.1}$$

5 Results and discussion

5.1 Verification of the s-CO_2 Brayton cycle model

The suitability of the Aspen Plus® model for simulating the performances of supercritical CO_2 Brayton cycles was investigated. An s-CO_2 recompression Brayton cycle (Figure 1b) was modelled for verifying the calculation. Independent results of numerical model reported by Dostal et al. [53] were compared with the Aspen Plus® simulation results. The input parameters were:

- Maximum cycle pressure - 200 bar
- Turbine inlet temperature - 550 ˚C
- Precooler outlet temperature - 32 ˚C
- Precooler outlet pressure - 76.92 bar
- Mass flow rate - 3176.4 kg/s
- MC pressure ratio - 2.6
- Split flow fraction - 0.41
- Turbine isentropic efficiency - 90 %
- Main and recompression compressors efficiency - 89 %

Comparison of the main simulation results against literature value is presented in Table 2. The maximum relative deviation is about 2.51%. The small differences in the result can be attributed to uncertainties in the pressure loss specifications and the round-off error in the input parameters. Otherwise, the simulation results agreed well with the literature values.

Table 2 Validation of s-CO_2 Brayton cycle model against literature value

Parameters	Literature value **[54]**	Simulation value	Relative difference
Turbine outlet temperature	440.29 ^{0}C	440.29 ^{0}C	0%
MC outlet temperature	61.1 ^{0}C	61.11 ^{0}C	0.02%
RC inlet temperature	69.59 ^{0}C	71.34 ^{0}C	2.51%
RC outlet temperature	157.99 ^{0}C	160.25 ^{0}C	1.43%
Heater inlet temperature	396.54 ^{0}C	397.38 ^{0}C	0.21%
Thermal power	600 MWt	596.76 MWt	0.54%
Turbine work	383.71 MW	383.72 MW	0.003%
MC work	38.59 MW	38.57 MW	0.05%
RC work	74.84 MW	75.84 MW	1.34%
Net work output	270.28 MW	269.31 MW	0.36%
HTR duty	985.51 MW	977.49 MW	0.81%
LTR duty	398.8 MW	398.0 MW	0.2%
Precooler duty	328.38 MW	328.11 MW	0.08%
Cycle efficiency	45.05%	45.13 %	0.08%

5.2 Baseline boundary conditions and design point parameters

The boundary conditions and parameters such as coal mass flow rate, combustion air conditions, percent excess air, flue gas stack temperature, maximum cycle pressure and turbines inlet temperature were selected based on the information published for the supercritical reheat steam cycle [45]. This will ensure a fair comparison between the performances of the s-CO_2 cycle plants and the conventional supercritical steam plant. Other conditions and parameters like pressure losses and specifications of heat exchangers were selected based on similar studies of s-CO_2 power cycle reported in the literature [15, 30]. A summary of the baseline boundary conditions and design point parameters is given in Table 3.

Table 3 Boundary conditions and design parameters

Parameter/variable	Value
Coal feed (^{0}C/bar/(kg/s))	15/1.01/51.82
Air (^{0}C/bar)	15/1.01
Excess air (%)	20
Maximum cycle pressure (bar)	290
HP & LP turbines inlet temperature (^{0}C)	593
Compressor inlet pressure (bar)	76
Compressor inlet temperature (^{0}C)	31
Gas-CO_2 TTD (^{0}C)	30
Preheater hot outlet temperature (^{0}C)	116
Recuperator TTD (^{0}C)	10
Turbine isentropic efficiency (%)	93
MC isentropic efficiency (%)	90
Recompression compressor isentropic efficiency (%)	89
Fan isentropic efficiency (%)	80
Generator efficiency (%)	98.4
Ash distribution, fly/bottom ash (%)	80/20

5.3 Performance comparisons among Cases A, B and C of the coal-fired s-CO_2 Brayton cycle power plants

The flow split fraction (i.e. the fraction of the total flow that goes through the precooler/main compressor) should be adjusted such that the differences in the heat capacities between the hot streams and the cold streams in recuperators are minimised. This will improve heat transfer in the recuperators and thereby maximised cycle efficiency. Figure 9 shows the cycle efficiencies as a function of the flow split fractions. The optimum flow split fraction was found to be about 0.65 for the topping cycle while it was about 0.71 for the single recuperator recompression bottoming cycle.

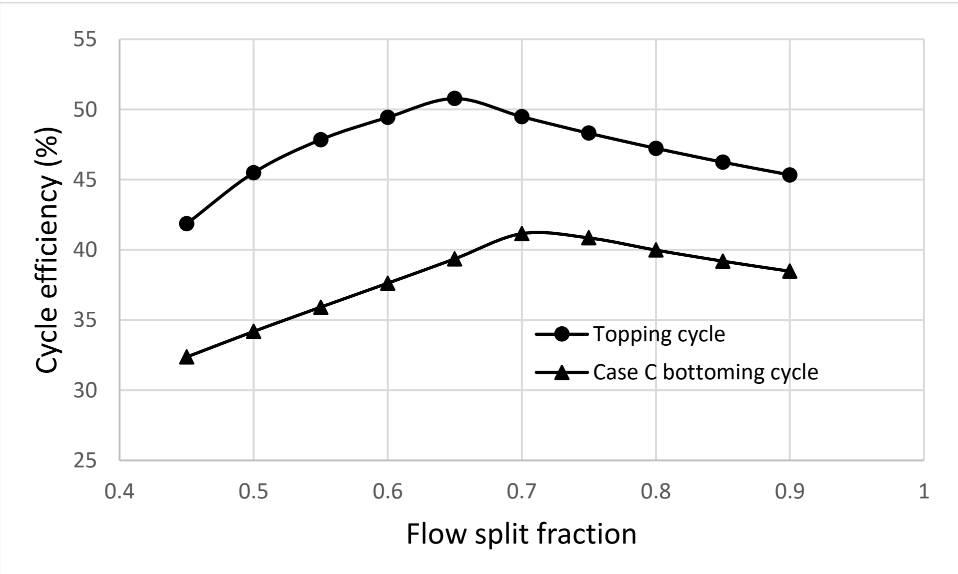

Figure 9 Cycle efficiencies of the topping cycle and Case C bottoming cycle as a function of the flow split fractions

In order to highlight the impact of integrating the coal-fired s-CO_2 power plants with the PCC unit, the performances of the power plants without carbon capture were first determined based the optimum flow split fractions, and the baseline boundary conditions and design parameters presented above. Table 4 shows the pressure, temperature and mass flow for the plants' main points. The stream nomenclature is based on Figure 3, Figure 4 and Figure 5. This was then followed by simulation and performance evaluation of the whole power plants, incorporating the PCC unit. The distribution of the fuel combustion heat energy among the different s-CO_2 heaters is shown in Figure 10. About 50% of the input heat energy was transferred by radiation to the s-CO_2 working fluid in the radiant heaters. The Case A and Case B bottoming cycles were able to recover about 12% of the total heat input, which otherwise would have been lost through the exhaust flue gas. In Case C, only about 9% was recovered but the unrecovered heat was utilised for preheating the secondary air to higher temperature level (258 ^{0}C) than Case A (177 ^{0}C) and Case B (165 ^{0}C). This then leads to higher heat transfer in the furnace for Case C. For the three cases, the heat losses were about 12%, that is, a furnace efficiency of approximately 88%. This value of furnace efficiency is comparable to the boiler efficiency obtainable in coal-fired steam power plants. Hence, the addition of the bottoming cycles and the combustion air preheaters enables efficient utilisation of the furnace heat.

Table 4 Summary of the main stream values for the three cases calculated with baseline boundary conditions and design parameters

	Case A			Case B			Case C		
Stream	P (bar)	T (^{0}C)	m (kg/s)	P (bar)	T (^{0}C)	m (kg/s)	P (bar)	T (^{0}C)	m (kg/s)
Coal	1.01	15	51.82	1.01	15	51.82	1.01	15	51.82
Air	1.01	15	540.88	1.01	15	540.88	1.01	15	540.88
Pry air	1.1	215	127.11	1.1	215	127.11	1.1	215	127.11
Sec. air	1.1	177.23	413.77	1.1	164.59	413.77	1.1	257.82	413.77
Pulv.Coal+air	1.09	75.28	178.93	1.09	75.28	178.93	1.09	75.28	178.93
A	1.09	1010	592.7	1.09	1010	592.7	1.09	1010	592.7
B	1.01	496	592.7	1.01	496	592.7	1.01	496	592.7
C	1.01	253.26	592.7	1.01	244.86	592.7	1.01	306.70	592.7
D	1.01	116	592.7	1.01	116	592.7	1.01	116	592.7
Flue to stack	1.01	56.67	585.08	1.01	56.67	585.08	1.01	56.67	585.08
T1	287.12	466	4052.52	287.12	466	4038.78	287.12	466	4163.13
T2	282.82	593	4052.52	282.82	593	4038.78	282.82	593	4163.13
T3	147.72	507.64	4052.52	147.72	507.64	4038.78	147.72	507.64	4163.13
T4	145.51	593	4052.52	145.51	593	4038.78	145.51	593	4163.13
a1,b1,c1	288.55	223.26	511.12	288.70	305.71	526.35	288.55	276.70	523.38
a2,b2,c2	287.25	466	511.12	287.25	466	526.35	287.25	466	523.38
b8	-	-	-	290	69.70	152.64	-	-	-

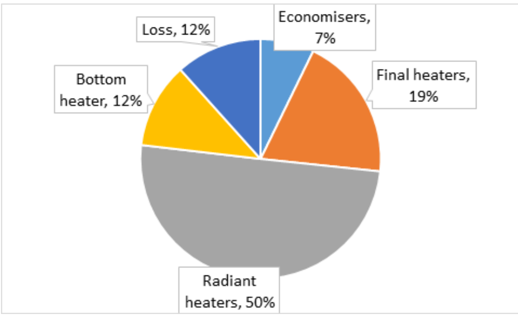

(a) Case A – Simple cycle bottoming

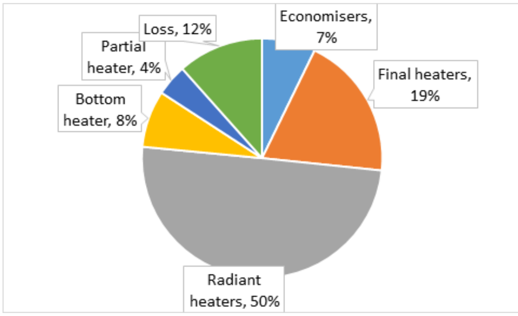

(b) Case B – Partial heating bottoming

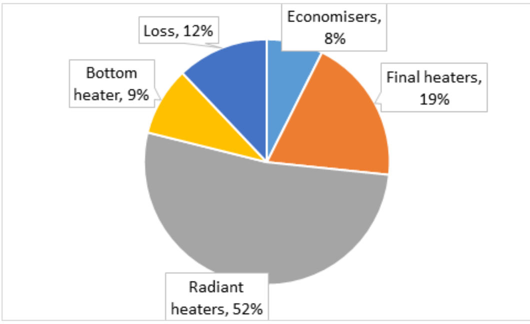

(c) Case C – Single recuperator recompression bottoming

Figure 10 Distribution of the input heat value among the different heaters

Table 5 shows the performance result of the PCC unit that was integrated with the coal-fired s-CO_2 Brayton cycle power plants. Integration of the PCC to the plants penalised the net efficiency through (1) bleeding of CO_2 for solvent regeneration in reboiler, which resulted in lower cycle efficiency (2) additional auxiliary loads associated with the PCC units. Table 6 is a summary of the performance results for the three cases both without the PCC unit and with the PCC unit integrated. Interestingly, Case C (i.e. the single recuperator recompression bottoming cycle layout) gave the best overall plant net efficiency with or without PCC even though the bottoming cycle recovered the least amount of heat and thus produced the least power. The superior performance of Case C is due to better efficiency of the bottoming cycle. In contrast, Kim et al. [15] concluded that power produced by bottoming cycle is a more important factor than the efficiency of bottoming cycle in determining the overall plant performance and therefore, did not recommend recompression cycle for bottoming cycle application despite having the best cycle efficiency. However, unlike our study, Kim et al. compared the performances of various s-CO_2 bottoming cycles without a downstream air preheater.

For a fixed coal fuel input, the plant overall performance depends on auxiliary loads, cycle efficiency and furnace efficiency. The cycle efficiency is majorly determined by the choice of cycle layout/configuration. Furnace efficiency, on the other hand, can be improved by heat recovery in the bottoming cycle and preheating of combustion air. In summary, the cycle layouts, the bottoming cycle heat recovery, the level of air preheating and the auxiliary loads will determine the plant net efficiency. Hence, for plants with similar auxiliary loads, plant net efficiency will be maximised by configurations with high cycle efficiency, good heat recovery in bottoming cycle and high level of air preheating. Unfortunately, good heat recovery in the bottoming cycle cannot be achieved simultaneously with a high level of air preheating. For instance, good heat recovery in the bottoming cycles of Case A and Case B meant that the temperature of the flue gas entering the air preheater was relatively low, limiting the amount of air preheating possible. On the other hand, Case C with the least heat recovery (or produced power) in bottoming cycle gave the highest air preheating duty (Table 6). Therefore, the poor heat recovery was somewhat compensated for by the added air preheater.

Table 5 Parameters and performance results of the PCC unit

Parameter	Value
CO_2 removal percentage	90%
Flue gas absorber inlet temperature	40 ^{0}C
Lean solvent absorber inlet temperature	40 ^{0}C
MEA concentration	30 wt.%
Absorber operating pressure	1.013 bar
Stripper operating pressure	1.9 bar
Lean solvent loading	0.29 mol CO_2/mol MEA
Rich solvent loading	0.53 mol CO_2/mol MEA
Reboiler temperature	120 ^{0}C
Condenser temperature	31.98 ^{0}C
Condenser duty	1.13 GJ/ton CO_2
Solvent circulation rate	18 m^3/ton CO_2
Reboiler duty	3.4 GJ/ton CO_2

Table 6 Comparison of plant performances with and without post-combustion CO_2 capture (PCC) for Case A (simple recuperative cycle as bottoming cycle), Case B (partial heating cycle as bottoming cycle) and Case C (single recuperator recompression cycle as bottoming cycle)

	Case A		Case B		Case C	
Parameter	No PCC	With PCC	No PCC	With PCC	No PCC	With PCC
HHV, MJ/kg	27.05	27.05	27.05	27.05	27.05	27.05
Input heat value, MJ	1401.87	1401.87	1401.87	1401.87	1401.87	1401.87
Heat transferred to top cycle, MW	1077.49	1103.16	1072.8	1095.63	1106.01	1131.81
Heat transferred to bottom cycle, MW	161.46	161.46	167.03	149.57	126.75	106.56
Furnace efficiency, %	88.38	88.74	88.44	88.82	87.94	88.34
Preheater duty, MW	92.61	59.80	87.18	51.15	127.43	96.14
Top gross electric power, MWe	545.40	401.98	543.31	398.08	560	416.32
Bottom gross electric power, MWe	60.17	46.39	61.96	48.95	52.61	39.58
Top cycle efficiency, %	50.62	36.44	50.64	36.33	50.63	36.78
Bottom cycle efficiency, %	37.27	32.94	37.10	32.73	41.51	37.14
Overall cycle efficiency, %	48.88	36.04	48.82	35.90	49.69	36.81
Auxiliaries power, MW	10.38	10.7	10.38	10.7	10.39	10.7
Net electric power, MWe	595.19	437.67	594.90	436.33	602.22	445.19
CO_2 specific emission, kg CO_2/MWh	714.69	98.05	715.04	98.35	706.35	96.39
Specific work output, kWh/m^3	5.28	5.24	5.26	5.23	5.16	5.10
Overall plant net efficiency, %	42.46	31.22	42.44	31.13	42.96	31.76

In Figure 11, the performances of the coal-fired s-CO_2 Brayton cycle power plants were compared with the state-of-the-art supercritical reheat steam power plant [51]. The s-CO_2 Brayton cycle power plants, without CO_2 capture, was found to be about 3.34 - 3.86% more efficient than the steam power plant. When the power plants were integrated with the PCC unit, the plant net efficiencies of the s-CO_2 power plants were about 0.68 – 1.31% above the steam plant's efficiency. Although the s-CO_2 Brayton cycle plants with CO_2 capture gave higher efficiency than steam cycle plant, the s-CO_2 cycle suffered more efficiency penalty (about 11.2%) than the steam plant (about 8.65%). This is probably due to the use of sensible heat of s-CO_2 working fluid to meet reboiler thermal requirement instead of low pressure condensing steam, as is usually the case in steam turbine power plant.

A comparison of the specific work output (i.e. the ratio of the generated power to the volumetric flow rate of the working fluid) of each cycle can give an indication of the relative size of plants and by extension the relative capital cost [20, 54]. Table 6 shows that the specific work outputs in all the three cases were comparable (approximately 5 kWh/m^3). Case C shows a slightly lower specific work output but the difference is not considered significant. The specific work output of the s-CO_2 cycle is over 30 times more than that of the steam cycle. Therefore, the s-CO2 cycle plant has the potential to be significantly smaller than the steam cycle plant. This is in good agreement with previous findings in the literature on the compactness of s-CO_2 cycle in comparison with steam cycle [11-13, 43].

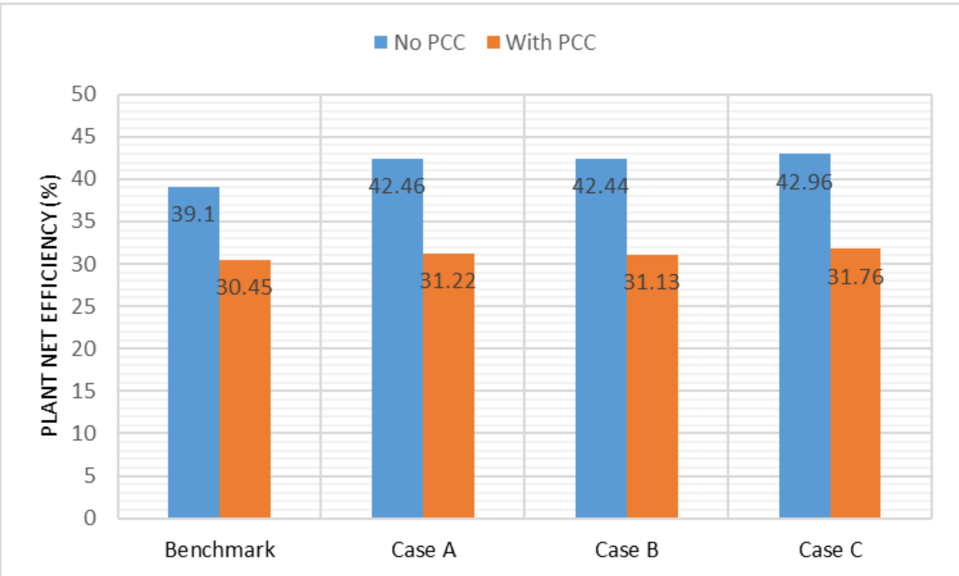

Figure 11 Comparison of the overall plant net efficiency of Case A (simple recuperative cycle as bottoming cycle), Case B (partial heating cycle as bottoming cycle) and Case C (single recuperator recompression cycle as bottoming cycle) with the supercritical steam plant (from Olaleye et al. [45]) as the benchmark

In this study, the cycle maximum pressure has been selected to match the maximum pressure in the steam cycle. However, a common feature of Brayton cycle is that there is an optimum pressure ratio (or cycle maximum pressure in our case) at which the efficiency has a peak value. Hence, the effect of cycle maximum pressure on plant performance was investigated by varying the pressure from 200 bar to 500 bar while the compressor inlet pressure was kept constant. Figure 12 shows the plant net efficiency as a function of cycle maximum pressure for the three configurations. Case C was found to maintain the best efficiency over the whole pressure range. Maximum efficiency occurred at an optimum pressure of about 400 bar.

Currently, the choice of such a high pressure might not be feasible due to mechanical design considerations such as the maximum pressure limit of heat exchangers, turbomachinery seal solutions to prevent leakage and the need to avoid excessively small compressor blades. However, the USC steam plant with a maximum pressure of 350 bar and a turbine inlet temperature of 700 ^{0}C is expected to come into operation between 2020 and 2030 [31]. If the s-CO_2 cycle is operated at such maximum pressure (i.e. 350 bar), a net efficiency gain up to 4.24% above the current efficiency of steam turbine plant can be achieved without a corresponding increase in turbine inlet temperature to 700 ^{0}C as planned. Hence, the s-CO_2 plant has the advantage of increased efficiency at a lower temperature.

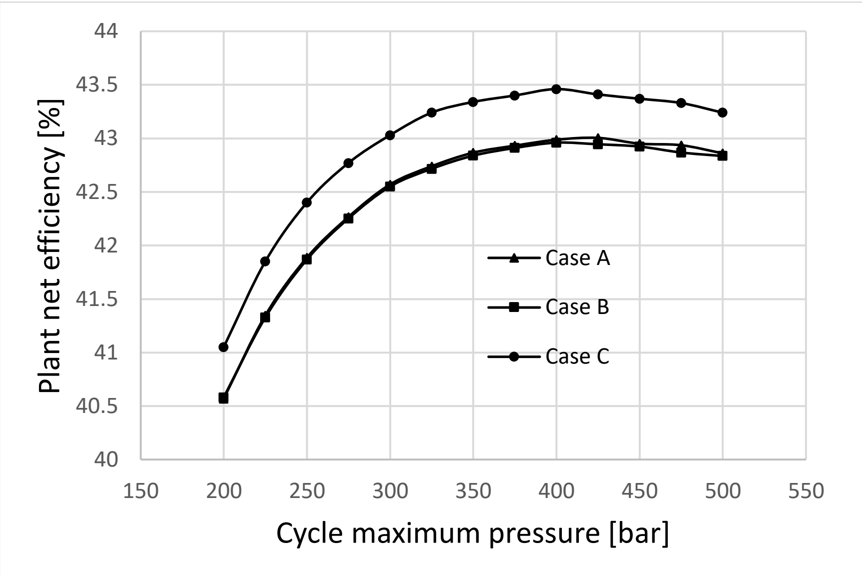

Figure 12 Plant net efficiency as a function cycle maximum pressure from 200 bar to 500 bar for the three configurations (Case A – simple recuperative cycle as bottoming cycle, Case B – partial heating cycle as bottoming cycle and Case C – single recuperator recompression cycle as bottoming cycle)

5.4 Choice of configuration and parametric study

In this study, the performance comparison was carried out for three potential s-CO_2 cycle configurations. The cycles were adapted for efficient utilisation of furnace heat similar to boiler heat utilisation in conventional steam turbine plant, albeit with bottoming cycles added. Operating conditions (290 bar, 593 ^{0}C and single reheat) were chosen to match the current supercritical steam cycle conditions. Hence, current experience with material technology for pulverised coal-fired boiler and steam turbine could be applied to the development of the coal-fired s-CO_2 Brayton cycle power plant. The overall net efficiency of Case C option without CO_2 capture was 0.5% and 0.52% over the efficiency of Case A and Case B respectively. With CO_2 capture, the efficiency gains were 0.54% and 0.63% above the efficiency of Case A and Case B respectively. Therefore, of the three alternative configurations considered, Case C (with single recuperator recompression cycle as the bottoming cycle) is more attractive due to its better performance. It is also expected to be of similar size as the other two configurations considering the relative value of the specific work output and the component count. When compared with steam cycle plant, the net efficiency of Case C was higher than the efficiency of steam cycle plant by about 3.86% and 1.31% without CO_2 capture and with CO_2 capture respectively.

Cycle efficiency is known to depend on the turbine inlet temperature, precooler outlet/main compressor inlet temperature and the recuperator minimum TTD. Hence, a parametric study was performed to investigate the effects of these parameters on the net efficiency of the chosen coal-fired s-CO_2 cycle power plant.

5.4.1 Effect of turbine inlet operation conditions

Figure 13 shows the effect of changes in turbine inlet temperature on the cycle performance for the single recuperator recompression bottoming cycle configuration without PCC unit and with PCC unit integrated. The figure was produced by varying the cycle maximum pressure from 200 bar to 500 bar for four different selection of turbine inlet temperatures (600 ^{0}C, 650 ^{0}C, 700 ^{0}C and 750 ^{0}C). The cycle performance was calculated with the flow split fraction that gave the maximum efficiency for each data point while other cycle parameters were maintained at the baseline condition.

The results showed that the plant net efficiency increased with the rise in turbine inlet temperature. Also for each selection of turbine inlet temperature, there is an optimum cycle maximum pressure. The optimum cycle maximum pressure increase with an increase of turbine inlet temperature. With no PCC and at a turbine inlet temperature of 600 ^{0}C, the optimum cycle maximum pressure was about 400 bar, while at 650 ^{0}C, the optimum cycle maximum cycle pressure increased to about 450 bar and the trend continued with increase in turbine inlet temperature. At the operating conditions of the next USC steam turbine power plant (700 ^{0}C and 350 bar), the efficiency of the s-CO_2 cycle power plant is about 46.67%. This corresponds to about 7.57% above the efficiency of the conventional supercritical steam plant.

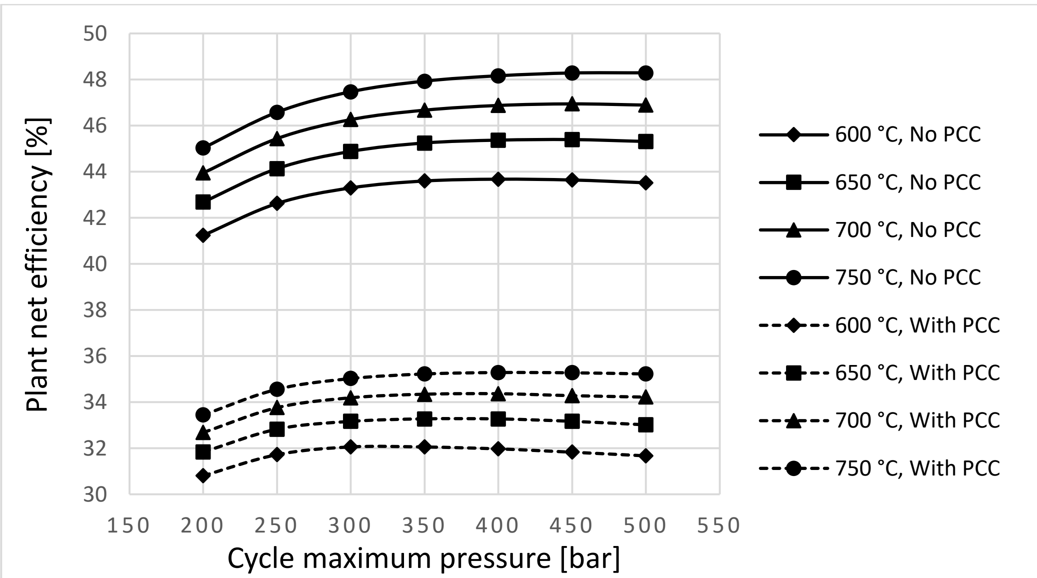

Figure 13 Plant net efficiency as a function of cycle maximum pressure at different turbine inlet temperature for the single recuperator recompression bottoming cycle configuration (i.e. Case C) with no carbon capture and with carbon capture integrated

From the foregoing, the adoption of the s-CO_2 cycle for coal-fired power plant application is promising. The s-CO_2 cycle achieved higher efficiency than steam cycle plant at similar operating conditions. Even for the advanced USC steam plant that is expected to achieve efficiency around 47%, this will be done with two or more reheat stages, three or more turbine modules and series of feedwater heaters. However, with potentially smaller footprint and less complex configuration, similar efficiency can be achieved with coal-fired s-CO_2 Brayton cycle power plant investigated in this study.

5.4.2 Effect of precooler outlet/main compressor inlet operating conditions

The selection of precooler outlet temperature (or main compressor inlet temperature) is based on the ambient or heat sink temperature, which depends on location as well as the type of cooling (wet cooling or dry cooling). The effect of precooler outlet operating conditions on cycle performance was investigated by varying the precooler outlet pressure from 60 bar to 110 bar for four selections of precooler outlet temperature (31, 34, 37 and 40 ^{0}C). In order to keep the cycle supercritical at all times, only values of precooler outlet temperature above CO_2 critical temperature was considered. The cycle efficiency was optimised with the flow split fraction while other parameters were fixed at the baseline value. Figure 14 shows the plant net efficiency as a function of precooler outlet temperature and pressure.

The plant net efficiency decreases with rise in precooler outlet temperature. However, for each precooler outlet temperature, there is a corresponding pseudo-critical pressure at which the plant efficiency is maximum. For instance, the highest plant net efficiency for a precooler outlet temperature of 31 ^{0}C was achieved at a precooler outlet pressure of 76 bar. However, when the precooler outlet temperature was increased to 34 ^{0}C, the optimum precooler outlet pressure also increased to 81 bar. This trend continued with increase in precooler outlet temperature. This is due to rapid rise of the density of the CO_2 working around the pseudo-critical pressures associated with the selected temperatures as shown in Figure 15. The increased density results in reduced compressor work and hence increased net work output or efficiency.

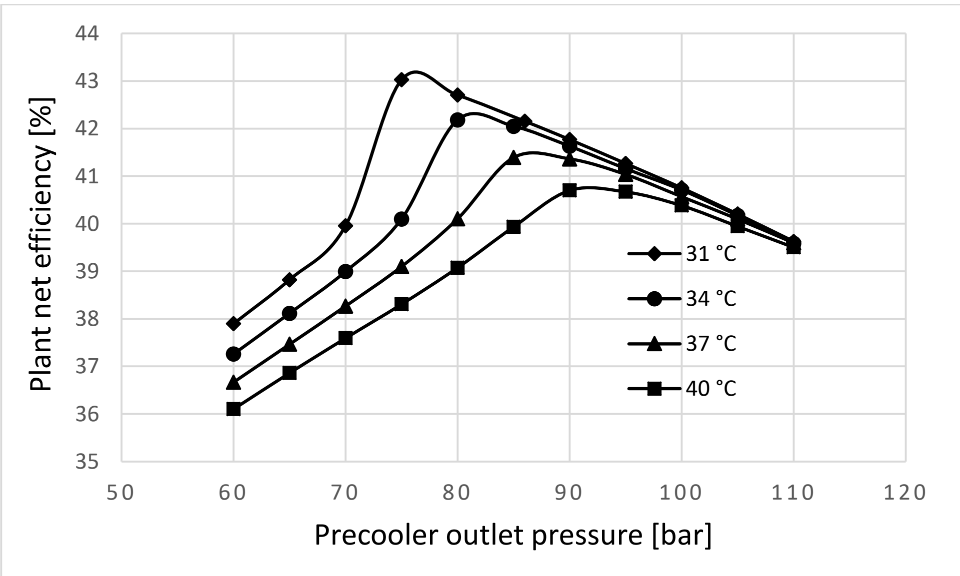

Figure 14 Effect of precooler outlet temperature on plant net efficiency of the single recuperator recompression bottoming cycle configuration with no carbon capture with precooler outlet pressure varying from 60 bar to 110 bar

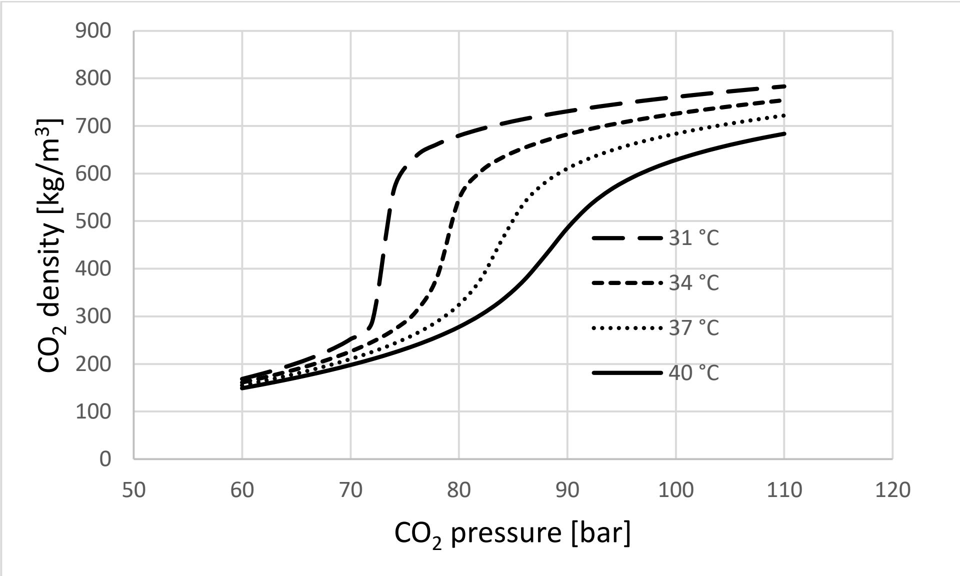

Figure 15 Plot of CO_2 pressure against density in the critical region showing the rapid rise in density at pseudo-critical pressures corresponding to different CO_2 temperatures

5.4.3 Effect of minimum terminal temperature difference of the recuperators

The minimum TTD of the recuperators is considered to be the smallest temperature difference between the hot and the cold stream at either hot inlet/cold outlet end or cold inlet/hot outlet end of the heat exchanger. Supercritical CO_2 recuperator is known to have pinch-point problem in which the smallest temperature difference occurs somewhere along the heat exchanger and not at the terminals [30]. The occurrence of pinch-point along the recuperator can be avoided by using recompression cycle and adjusting the flow split fractions to balance the heat capacities of the hot and cold stream. Therefore, minimum TTD will be the same as pinch-point temperature difference if the pinch-point is located at the terminal of the recuperators.

The selection of recuperator TTD or pinch-point temperature difference will influence the cycle efficiency and size of the recuperator [30]. Previous studies showed that the recuperator constituted the largest percentage of the size of closed Brayton cycle plant [17, 55]. For the coal-fired s-CO_2 cycle plant with single recuperator recompression bottoming cycle, the effect of the recuperators' minimum TTD on the plant net efficiency is shown in Figure 16. The plant net efficiency decreased with increasing minimum TTD of the recuperators. For every 1^0C increase in minimum TTD, the net efficiency was reduced by approximately 0.17%. Hence, improved plant performance can be achieved by reducing the TTD between the hot and cold stream. This is because reducing the TTD will improve the effectiveness of the recuperator, and thus the plant performance. However, this will be at the cost of increased size of recuperator because more heat transfer area will be required.

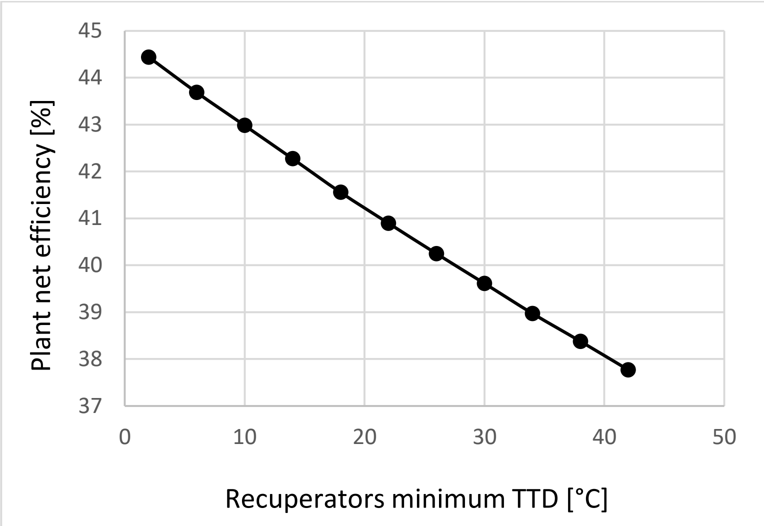

Figure 16 Plant net efficiency as a function of recuperators minimum TTD for the single recuperator recompression bottoming cycle s-CO_2 plant

6 Conclusions

In this paper, s-CO_2 Brayton cycle has been proposed as a potential replacement for steam Rankine cycle of coal-fired power plant with solvent-based post-combustion CO_2 capture. Performance evaluation shows that the s-CO_2 Brayton cycle can be adapted for efficient utilisation of furnace and flue gases heat by using a topping s-CO_2 cycle and a bottoming s-CO_2 cycle in addition to combustion air preheating. The coal-fired s-CO_2 cycle is able to achieve furnace efficiency of about 88% in the three cases, which is comparable to the boiler efficiency of the conventional supercritical steam plant. The plant net efficiency of the s-CO_2 Brayton cycle plant without CO_2 capture is about 3.34-3.86% more than that of the supercritical steam plant. With CO_2 capture, the coal-fired s-CO_2 cycle suffers an efficiency penalty of about 11.2%, which is more than the efficiency penalty of the reference supercritical steam cycle plant (8.65%). Nevertheless, the plant net efficiency of the s-CO_2 cycle plant is still about 0.68-1.31% more than that of the supercritical steam cycle with PCC. For the three investigated cases, Case C (newly proposed bottoming cycle) is the most attractive configuration as it gives the highest plant net efficiency either without or with CO_2 capture. Also, comparison of the specific work outputs indicates that the size of the new concept is not expected to be significantly larger than those of Case A and Case B.

Taken together, these findings suggest that cascaded s-CO_2 Brayton cycle is a promising power conversion system for coal-fired power plant application. The current study is conceptual in nature. Nevertheless, it provides considerable insight into the thermodynamic performance of s-CO_2 Brayton cycle adapted for coal-fired power plant, employing a topping reheat recompression s-CO2 cycle and different options of bottoming s-CO_2 cycles. Operating conditions have been chosen to be similar to conditions obtainable in the current supercritical steam boiler so that the current experience with boiler material technology can be applied to the s-CO_2 furnace. Therefore, future development efforts can be focused on the s-CO_2 Brayton cycles.

Acknowledgements

This work was supported financially by GE Power (formerly ALSTOM Power Ltd) and the EU FP7 Marie Curie (grant number: R-D-CSPP-PSE PIRSES-GA-2013-612230).

References

[1] International Energy Agency (IEA), "Key world energy trends: Excerpt from world energy balances," International Energy Agency, Paris, France, 2016, Available: http://www.iea.org/publications/freepublications/publication/KeyWorldEnergyTrends.pdf, Accessed on: 15 March 2017.

[2] G. Cau, V. Tola, and C. Bassano, "Performance evaluation of high-sulphur coal-fired USC plant integrated with SNOX and CO2 capture sections," Applied Thermal Engineering, vol. 74, pp. 136-145, 2015.

[3] Intergovernmental Panel on Climate Change (IPCC), "IPCC Special Report: Carbon Dioxide Capture and Storage," in "A Special Report of Working Group III of the Intergovernmental Panel on Climate Change," Intergovernmental Panel on Climate Change, Geneva, Switzerland, 2005, Available: https://www.ipcc.ch/report/srccs/, Accessed on: 10 February 2017.

[4] U. S. P.R.Arachchige and M. C. Melaaen, "Aspen Plus Simulation of CO2 Removal from Coal and Gas Fired Power Plants," Energy Procedia, vol. 23, pp. 391-399, 2012.

[5] K. Goto, K. Yogo, and T. Higashii, "A review of efficiency penalty in a coal-fired power plant with post-combustion CO2 capture," Applied Energy, vol. 111, pp. 710-720, 2013.

[6] E. J. Parma et al., "Supercritical CO2 Direct Cycle Gas Fast Reactor (SC-GFR) Concept," in Proceedings of the Supercritical CO2 Power Cycle Symposium, Boulder, Colorado, 2011.

[7] G. Manente and A. Lazzaretto, "Innovative biomass to power conversion systems based on cascaded supercritical CO2 Brayton cycles," Biomass and Bioenergy, vol. 69, no. 0, pp. 155-168, 2014.

[8] H. S. Pham et al., "Mapping of the thermodynamic performance of the supercritical CO2 cycle and optimisation for a small modular reactor and a sodium-cooled fast reactor," Energy, vol. 87, pp. 412-424, 2015.

[9] J. J. Pasch, T. M. Conboy, D. D. Fleming, and G. E. Rochau, "Supercritical CO2 recompression Brayton cycle: completed assembly description," Sandia National Laboratories, Albuquerque, California, 2012.

[10] E. G. Feher, "The supercritical thermodynamic power cycle," in IECEC Meeting, Douglas Paper No. 4348, Miami Beach, Florida, 1967: IECEC.

[11] V. Dostal, "A supercritical carbon dioxide cycle for next generation nuclear reactors," PhD Thesis, Massachusetts Institute of Technology (MIT), Cambridge, Massachusetts, USA, 2004.

[12] G. Angelino, "Carbon dioxide condensation cycles for power production," Journal of Engineering for Gas Turbines and Power, vol. 90, no. 3, pp. 287-295, 1968.

[13] S. Ishiyama, Y. Muto, Y. Kato, S. Nishio, T. Hayashi, and Y. Nomoto, "Study of steam, helium, and supercritical CO2 turbine power generations in prototype fusion power reactor," Progress in Nuclear Energy, vol. 50, no. 2-6, pp. 325-332, 2008.

[14] V. T. Cheang, R. A. Hedderwick, and C. McGregor, "Benchmarking supercritical carbon dioxide cycles against steam Rankine cycles for Concentrated Solar Power," Solar Energy, vol. 113, no. 0, pp. 199-211, 2015.

[15] M. S. Kim, Y. Ahn, B. Kim, and J. I. Lee, "Study on the supercritical CO2 power cycles for landfill gas firing gas turbine bottoming cycle," Energy, vol. 111, pp. 893-909, 2016.

[16] D. P. Hanak and V. Manovic, "Calcium looping with supercritical CO2 cycle for decarbonisation of coal-fired power plant," Energy, vol. 102, pp. 343-353, 2016.

[17] L. Hu et al., "Investigation on the performance of the supercritical Brayton cycle with CO2-based binary mixture as working fluid for an energy transportation system of a nuclear reactor," Energy, vol. 89, pp. 874-886, 2015.

[18] H. Li, Y. Zhang, L. Zhang, M. Yao, A. Kruizenga, and M. Anderson, "PDF-based modeling on the turbulent convection heat transfer of supercritical CO2 in the printed circuit heat exchangers for the supercritical CO2 Brayton cycle," International Journal of Heat and Mass Transfer, vol. 98, pp. 204-218, 2016.

[19] Y. Ahn et al., "Review of supercritical CO2 power cycle technology and current status of research and development," Nuclear Engineering and Technology, vol. 47, no. 6, pp. 647-661, 2015.

[20] S. J. Bae, Y. Ahn, J. Lee, and J. I. Lee, "Various supercritical carbon dioxide cycle layouts study for molten carbonate fuel cell application," Journal of Power Sources, vol. 270, pp. 608-618, 2014.

[21] G. Sulzer, "Verfahren zur Erzeugung von Arbeit aus Warme," Patent Swiss Patent CH 269599, 1950.

[22] E. G. Feher, "Supercritical cycle heat engine," Patent Patent US3237403, 1966.

[23] G. Angelino, "Real gas effects in carbon dioxide cycles," in ASME 1969 Gas Turbine Conference and Products Show, 1969, pp. V001T01A071-V001T01A071: American Society of Mechanical Engineers.

[24] V. L. Dekhtiarev, "On designing a large, highly economical carbon dioxide power installation," Elecrtichenskie Stantskii, vol. 5, no. 5, pp. 1-6, 1962.

[25] L. Santini, C. Accornero, and A. Cioncolini, "On the adoption of carbon dioxide thermodynamic cycles for nuclear power conversion: A case study applied to Mochovce 3 Nuclear Power Plant," Applied Energy, vol. 181, pp. 446-463, 2016.

[26] O. Olumayegun, M. Wang, and G. Kelsall, "Closed-cycle gas turbine for power generation: A state-of-the-art review," Fuel, vol. 180, no. 0, pp. 694-717, 2016.

[27] F. Crespi, G. Gavagnin, D. Sánchez, and G. S. Martínez, "Supercritical carbon dioxide cycles for power generation: A review," Applied Energy, vol. 195, no. 0, pp. 152-183, 2017.

[28] M.-J. Li, H.-H. Zhu, J.-Q. Guo, K. Wang, and W.-Q. Tao, "The development technology and applications of supercritical CO2 power cycle in nuclear energy, solar energy and other energy industries," Applied Thermal Engineering, vol. 126, no. Supplement C, pp. 255-275, 2017.

[29] T. Neises and C. Turchi, "A Comparison of Supercritical Carbon Dioxide Power Cycle Configurations with an Emphasis on CSP Applications," Energy Procedia, vol. 49, pp. 1187-1196, 2014.

[30] M. Mecheri and Y. Le Moullec, "Supercritical CO2 Brayton cycles for coal-fired power plants," Energy, vol. 103, pp. 758-771, 2016.

[31] Y. Le Moullec, "Conceptual study of a high efficiency coal-fired power plant with CO2 capture using a supercritical CO2 Brayton cycle," Energy, vol. 49, no. 0, pp. 32-46, 2013.

[32] R. Chacartegui, J. M. Muñoz de Escalona, D. Sánchez, B. Monje, and T. Sánchez, "Alternative cycles based on carbon dioxide for central receiver solar power plants," Applied Thermal Engineering, vol. 31, no. 5, pp. 872-879, 2011.

[33] F. A. Al-Sulaiman and M. Atif, "Performance comparison of different supercritical carbon dioxide Brayton cycles integrated with a solar power tower," Energy, vol. 82, pp. 61-71, 2015.

[34] K. Wang, Y.-L. He, and H.-H. Zhu, "Integration between supercritical CO2 Brayton cycles and molten salt solar power towers: A review and a comprehensive comparison of different cycle layouts," Applied Energy, vol. 195, pp. 819-836, 2017.

[35] M. Persichilli, T. Held, S. Hostler, E. Zdankiewicz, and D. Klapp, "Transforming waste heat to power through development of a CO2-based power cycle," in Proceedings of Electric Power Expo, Rosemount, IL, U.S.A., 2011.

[36] S. Banik, S. Ray, and S. De, "Thermodynamic modelling of a recompression CO2 power cycle for low temperature waste heat recovery," Applied Thermal Engineering, vol. 107, pp. 441-452, 2016.

[37] Y. Muto and Y. Kato, "Optimal cycle scheme of direct cycle supercritical CO2 gas turbine for nuclear power generation systems," Journal of Power and Energy Systems, vol. 2, no. 3, pp. 1060-1073, 2008.

[38] A. Moisseytsev and J. J. Sienicki, "Investigation of alternative layouts for the supercritical carbon dioxide Brayton cycle for a sodium-cooled fast reactor," Nuclear Engineering and Design, vol. 239, no. 7, pp. 1362-1371, 2009.

[39] O. Olumayegun, M. Wang, and E. Oko, "Thermodynamic performance evaluation of supercritical CO_2 closed Brayton Cycles for coal-fired power generation with post-combustion carbon capture," presented at the 11th ECCRIA (European Conference on Coal Research and its Applications), The University of Sheffield, Sheffield, UK, 5-7 September, 2016. Available: http://www.maggichurchouseevents.co.uk/ferf/downloads/1B3%20Olumayegun%20Olumide.pdf

[40] T. M. Conboy, S. A. Wright, D. E. Ames, and T. G. Lewis, "CO2-based mixtures as working fluids for geothermal turbines," Sandia National Laboratories (SNL), Albuquerque, New Mexico, SAND2012-4905, 2012, Available: http://prod.sandia.gov/techlib/access-control.cgi/2012/124905.pdf.

[41] B. G. Miller, Clean coal engineering technology. Boston: Butterworth-Heinemann, 2011.

[42] T. Fout et al., "Cost and performance baseline for fossil energy plant (Volume 1a): Bituminous coal (PC) and natural gas to electricity (Revision 3)," National Energy Technology Laboratory (NETL), Pittsburgh, PA, DOE/NETL-2015/1723, 2015, Available: https://www.netl.doe.gov/File%20Library/Research/Energy%20Analysis/Publications/Rev3Vol1aPC_NGCC_final.pdf.

[43] O. Olumayegun, M. Wang, and G. Kelsall, "Closed-cycle gas turbine for power generation: A state-of-the-art review," Fuel, vol. 180, pp. 694-717, 2016.

[44] Reuters. (2014). Echogen Power Systems' waste heat recovery system available as turnkey solution. Available: http://uk.reuters.com/article/2014/12/08/idUSnMKWcgTnHa+1ca+MKW20141208

[45] A. K. Olaleye, M. Wang, and G. Kelsall, "Steady state simulation and exergy analysis of supercritical coal-fired power plant with CO2 capture," Fuel, vol. 151, pp. 57-72, 2015.

[46] F. Emun, M. Gadalla, T. Majozi, and D. Boer, "Integrated gasification combined cycle (IGCC) process simulation and optimization," Computers & Chemical Engineering, vol. 34, no. 3, pp. 331-338, 2010.

[47] AspenTech, "Aspen Plus: Getting started modeling processes with solids," Aspen Technology, Inc., Burlington, MA, 2013.

[48] E. W. Lemmon, M. L. Huber, and M. O. McLinden, "NIST Standard Reference Database 23: Reference Fluid Thermodynamic and Transport Properties-REFPROP," Version 9.1 ed. Gaithersburg: National Institute of Standards and Technology (NIST), 2013.

[49] N. A. Carstens, "Control Strategies for Supercritical Carbon Dioxide Power Conversion Systems," PhD Thesis, Massachusetts Institute of Technology (MIT), Cambridge, Massachusetts, USA, 2007.

[50] P. K. Nag, Power plant engineering. New Delhi: Tata McGraw-Hill, 2008.

[51] Y. Zhang, H. Chen, C.-C. Chen, J. M. Plaza, R. Dugas, and G. T. Rochelle, "Rate-Based Process Modeling Study of CO2 Capture with Aqueous Monoethanolamine Solution," Industrial & Engineering Chemistry Research, vol. 48, no. 20, pp. 9233-9246, 2009.

[52] Y. Zhang and C.-C. Chen, "Modeling CO2 Absorption and Desorption by Aqueous Monoethanolamine Solution with Aspen Rate-based Model," Energy Procedia, vol. 37, pp. 1584-1596, 2013.

[53] V. Dostal, M. J. Driscoll, and P. Hejzlar, "A supercritical carbon dioxide cycle for next generation nuclear reactors," The MIT Centre for Advanced Nuclear Energy Systems, Cambridge, Massachusetts (USA), MIT-ANP-TR-100, 2004, Available: http://web.mit.edu/22.33/www/dostal.pdf.

[54] H. I. H. Saravanamuttoo, G. F. C. Rogers, H. Cohen, and P. Straznicky, Gas Turbine Theory, 6th ed. Essex (UK): Prentice Hall, Pearson Education, 2009.

[55] O. Olumayegun, M. Wang, and G. Kelsall, "Thermodynamic analysis and preliminary design of closed Brayton cycle using nitrogen as working fluid and coupled to small modular Sodium-cooled fast reactor (SM-SFR)," Applied Energy, vol. 191, pp. 436-453, 2017.